Rivelatori per neutrini (extra)galattici di altissime energie

Reazioni tipiche:

ν_μ + N $\rightarrow$ μ^- + adroni
ν_e + N $\rightarrow$ e^- + adroni

Piccolissime sezioni d'urto $\rightarrow$ necessari enormi volumi di materiale per avere un ragionevole numero di eventi

Nei primi rivelatori sviluppati/in costruzione: solo misura del μ nella prima delle reazioni. Rivelazione dell'elettrone possibile, ma relativa efficienza bassa.

Importante uno studio dettagliato delle caratteristiche di propagazione del μ nella roccia/acqua/ghiaccio$\rightarrow$

Perdite d'energia dei μ underground

Profondita' atmosferica: X ~ 1000 g x cm^{-2}
Sotto 1 km di roccia: X → 2.65 x 10^5 g x cm^{-2}
Spesso espressa in km di acqua equivalente (1 km a.e.=10^5 g x cm^{-2})
A densita' cosi' elevate il μ subisce, oltre alla perdita d'energia per ionizzazione (all'incirca indipendente dall'energia e pari a circa 2 MeV g^{-1} cm^2), anche:
-bremsstrahlung
-produzione di coppie elettrone-positrone
-fotoproduzione
Questi sono proporzionali all'energia →

$$\frac{dE}{dx} = -a - bE_\mu$$

$$b = b_{br} + b_{pair} + b_{ph}; \qquad \text{Roccia}: b \cong 4 \times 10^{-6} \quad \left(g^{-1}\, cm^2\right)$$

Energia critica ⇒ perdita d'energia per ionizzazione = perdita d'energia per processi radiativi:

$$a = bE_\mu \Rightarrow E_{cr} = \frac{a}{b} \equiv \varepsilon \cong 500\ GeV$$

Perdita d'energia dominata da effetti radiativi per E_μ molto maggiore di ε

Perdita d'energia dominata da ionizzazione per E_μ molto minore di ε

Contributi relativi alla perdita d'energia per radiazione dei μ undeground

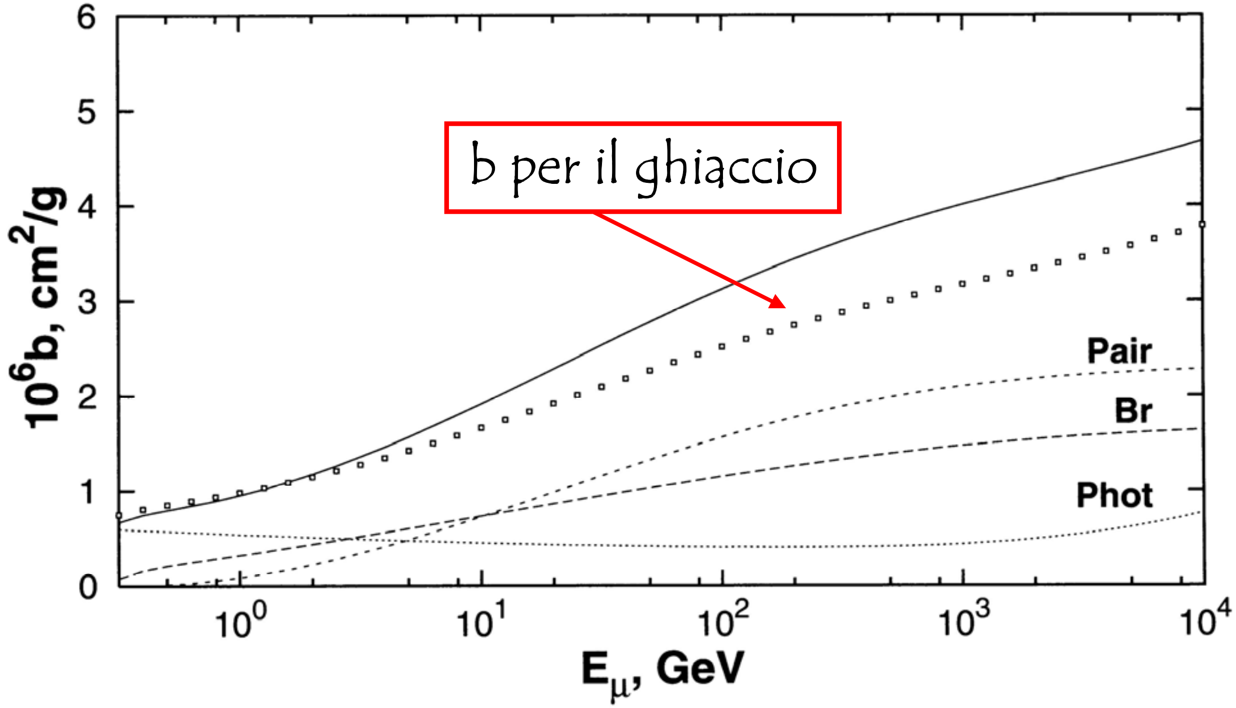

Fig. 7.4. Relative energy loss on radiation in standard rock. Solid line shows the sum of the three processes. Circles show the b value for clean ice.

Perdite d'energia dei μ underground

$$\frac{dE}{dx} = -a - bE_\mu$$

$$E_{cr} = \frac{a}{b} \equiv \varepsilon \cong 500\ GeV$$

Energia di un μ avente energia iniziale E_μ^0 dopo un percorso X nella roccia :

$$E_\mu(X) = \left(E_\mu^0 + \varepsilon\right) \times e^{-bX} - \varepsilon \quad \Rightarrow E_\mu^0 = E_\mu \times e^{bX} + \varepsilon\left(e^{bX} - 1\right)$$

Minima energia che un μ deve avere per penetrare ad una profondita' X :

$$\left(E_\mu^{\min} + \varepsilon\right) \times e^{-bX} - \varepsilon = 0 \Rightarrow E_\mu^{\min} = \varepsilon\left[e^{bX} - 1\right]$$

Per piccole profondita' $(bX << 1)$, sviluppando l'esponenziale $\Rightarrow E_\mu^{\min} = \varepsilon\left[1 + bX - 1\right] = aX$

Cioe' la perdita d'energia avviene sopratutto per ionizzazione.

Spettro osservato dei μ ad una profondita' X :

$$\frac{dN}{dE_\mu} = \frac{dN}{dE_\mu^0} \times \frac{dE_\mu^0}{dE_\mu} = \frac{dN}{dE_\mu^0} e^{bX}$$ che, per $X >> 1/b$ riproduce lo spettro in superficie.

Per $E_\mu << \varepsilon \Rightarrow E_\mu = E_\mu^0 \text{-} aX$ e quindi :

$$\frac{dN}{dE_\mu} = \frac{dN}{dE_\mu^0}$$ per $E_\mu > aX$; per $E_\mu \leq aX$ lo spettro risulta appiattito.

Flusso di μ underground

Relazione profondita'-flusso: flusso dei μ in funzione di X

Flusso al suolo :

$$F_\mu = K \times E_\mu^{-\alpha}$$

Relazione Profondita'-Intensita' (Flusso a profondita' X) :

$$F_\mu^{vert} = \frac{K\varepsilon^{-\alpha+1}}{\alpha - 1} \times \exp\left[-(\alpha - 1)bX\right] \times \left(1 - e^{-bX}\right)^{-\alpha+1}$$

Flusso di μ underground

Relazione profondita'-flusso: flusso dei μ in funzione di X
Misure da esperimenti diversi, tradotte in flusso di μ lungo la verticale in "acqua"

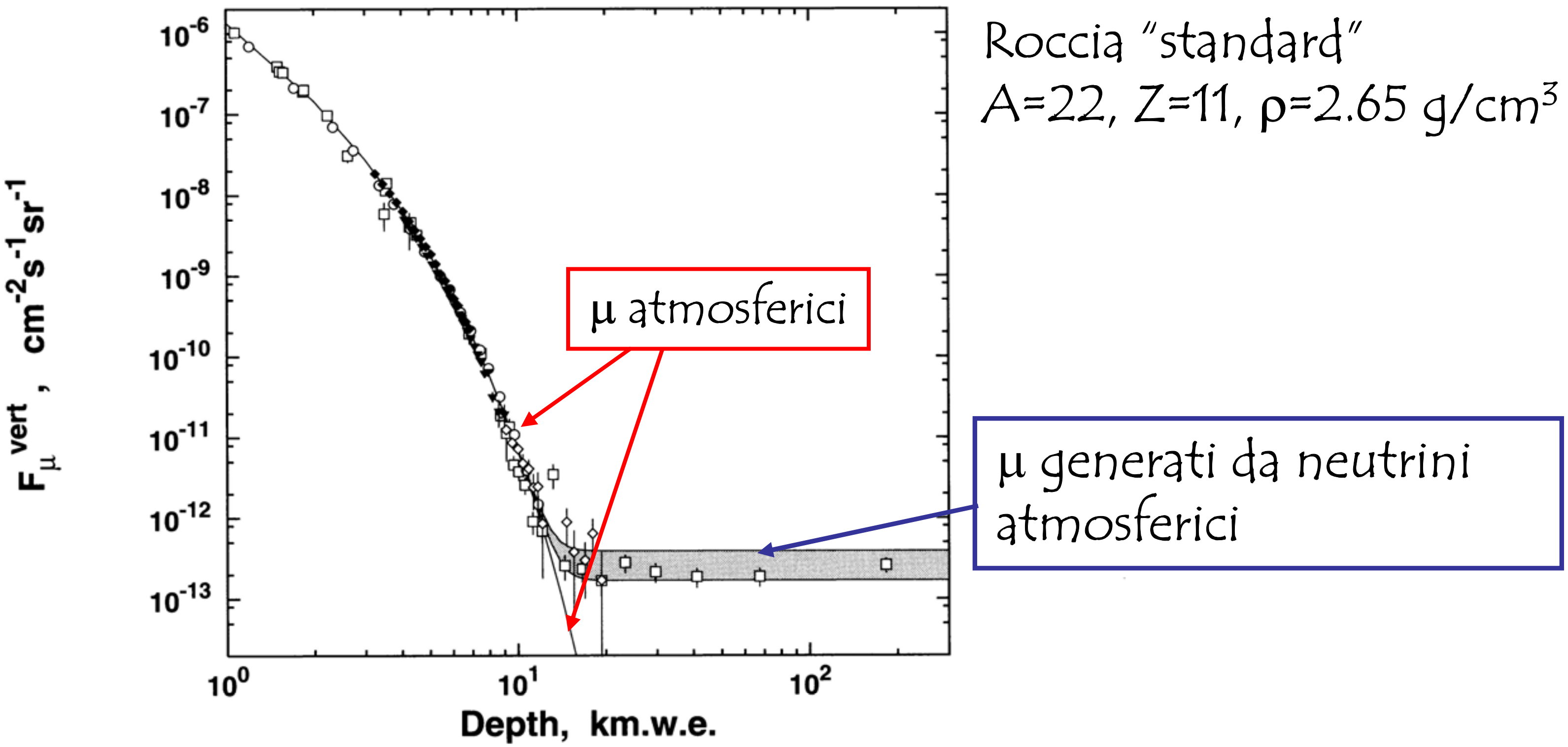

Roccia "standard"
A=22, Z=11, ρ=2.65 g/cm^3

Fig. 7.1. Depth–intensity relation – the integral muon flux measured at different depths and angles and converted to vertical muon flux is compared to predictions. See text for the references to different data sets.

Perdite d'energia dei μ underground

Range di un μ:

$$R(E_\mu) = \frac{1}{b}\ln\left(\frac{E_\mu}{\varepsilon}+1\right)$$

Ipotesi che la perdita d'energia sia continua (ionizzazione). Cioe' fino a circa 100 GeV.

Non vera per i processi radiativi (dominati da pochi eventi con grosse perdite d'energia.

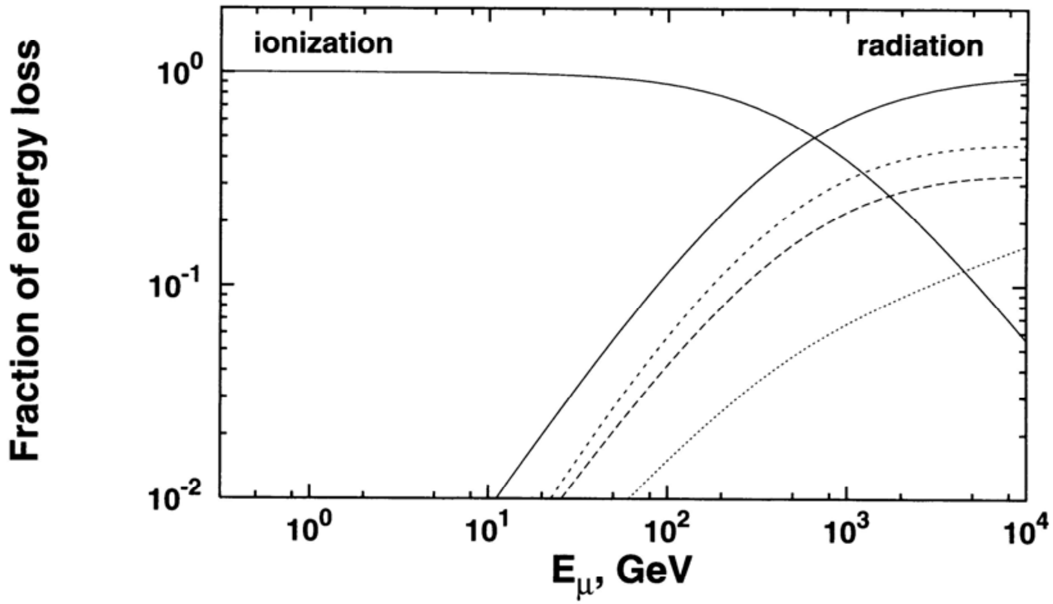

Fig. 7.2. Relative importance of different radiation processes as a function of the muon energy normalized to the total energy loss per g/cm^2. The long-dashed curve is for bremsstrahlung, the short-dashed curve for direct pair-production, and the dotted curve for photoproduction.

Probabilita' di penetrazione dei μ underground

Mesoni μ che non subiscono processi radiativi possono propagarsi molto oltre la profondita' X.
Confronto di $\langle R_\mu \rangle$ con R. Rapporto $\langle R_\mu \rangle / R$ dipende dall'energia.
Nella pratica si ricorre a simulazioni MC piuttosto che al calcolo analitico.

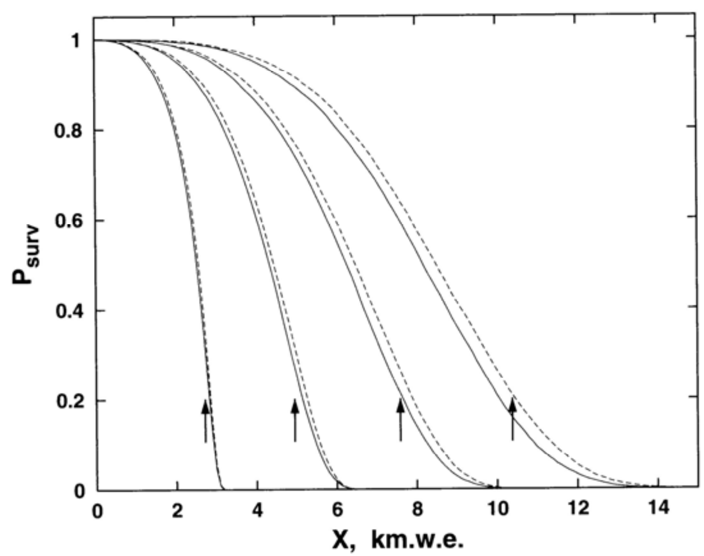

Fig. 7.3. Survival probability of muons with energy of 1., 3.16, 10., and 31.6 TeV in standard rock. The two curves for each energy indicate the uncertainties in the bremsstrahlung cross-section as stated in below. The arrows show the average depth for muon survival calculated from (7.4).

Neutrini cosmici

Neutrini osservati nella radiazione cosmica:

a) dal Sole
b) dalla SN1987A
   Energie di pochi MeV
c) dai raggi cosmici (decadimenti dei π)

Energie fino a qualche decina di GeV

Osservazione di neutrini di alte energie da sorgenti Galattiche ?

Vantaggi dei neutrini:

a) poco assorbiti dal materiale della sorgente in cui sono prodotti → informazioni sul nucleo della sorgente
b) poco assorbiti dal mezzo Galattico/Intergalattico
c) non deflessi da campi magnetici

Fotoni fortemente assorbiti per energie superiori a 10^{13} eV (interazione con il CMB)

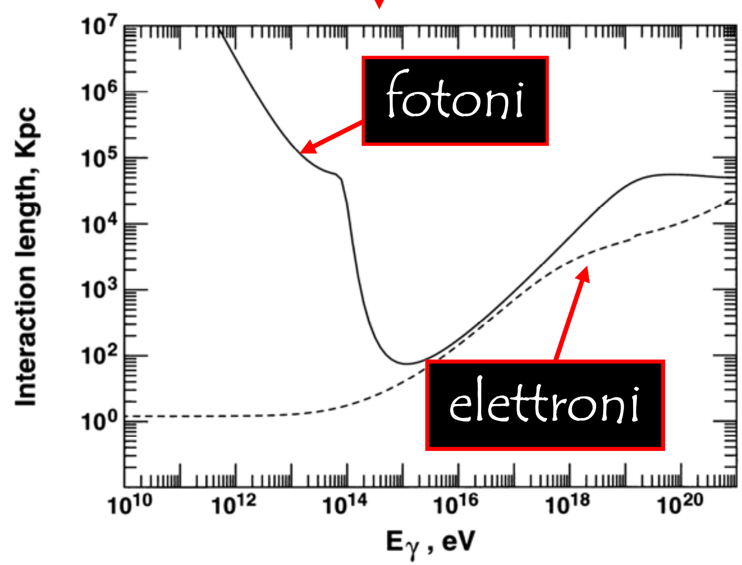

Fig. 10.1. Interaction length for γ-ray (solid) and electron (dashed line) interactions on the universal photon backgrounds. Only the major process of production of electron–positron pairs is plotted for gamma-rays. The electron interaction length is shown for inverse Compton effect.

Neutrini cosmici

Inoltre i neutrini possono aiutarci a discriminare tra modelli di produzione adronica/leptonica in SN, AGN, etc.

Svantaggi dei neutrini:
piccola sezione d'urto, anche ad alte energie (circa 10 ordini di grandezza inferiore a quella dei fotoni)

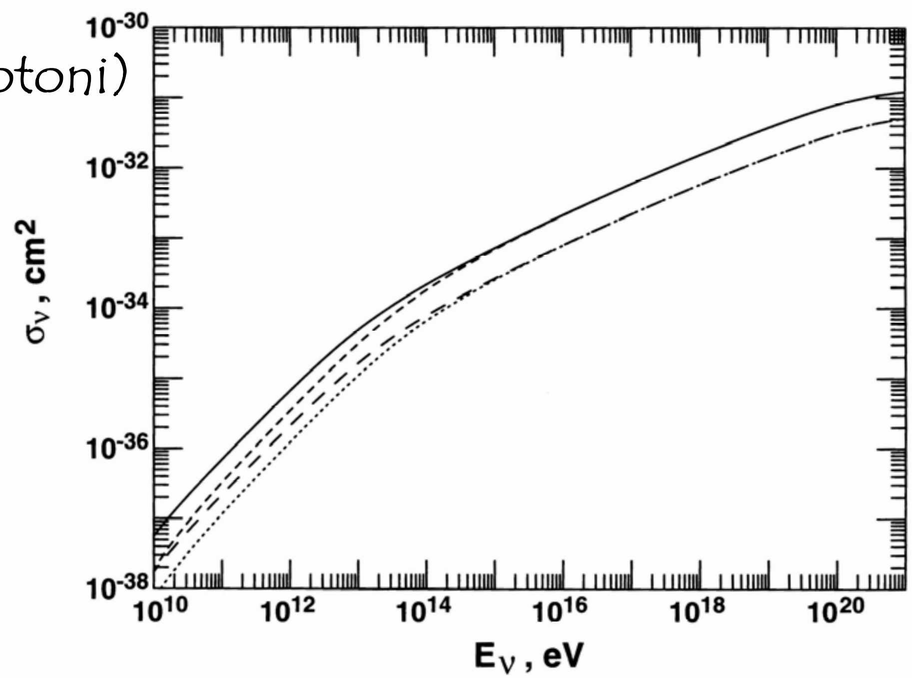

Fig. 10.2. Cross-sections for deep inelastic neutrino scattering. Neutrino CC cross-section is plotted with a solid line, the antineutrino with short dashes. The NC cross-section for neutrinos are plotted with long dashes, and for antineutrinos with a dotted line.

Neutrini cosmici

Neutrini prodotti in oggetti Galattici/Extragalattici:

$p + p \rightarrow p(n) + m\,\pi^0 + 2m\,\pi^{+/-}$

$\pi^{+/-} \rightarrow \mu^{+/-}\,\nu$

$\pi^0 \rightarrow \gamma\,\gamma$

Produzione di neutrini e fotoni in sistemi binari

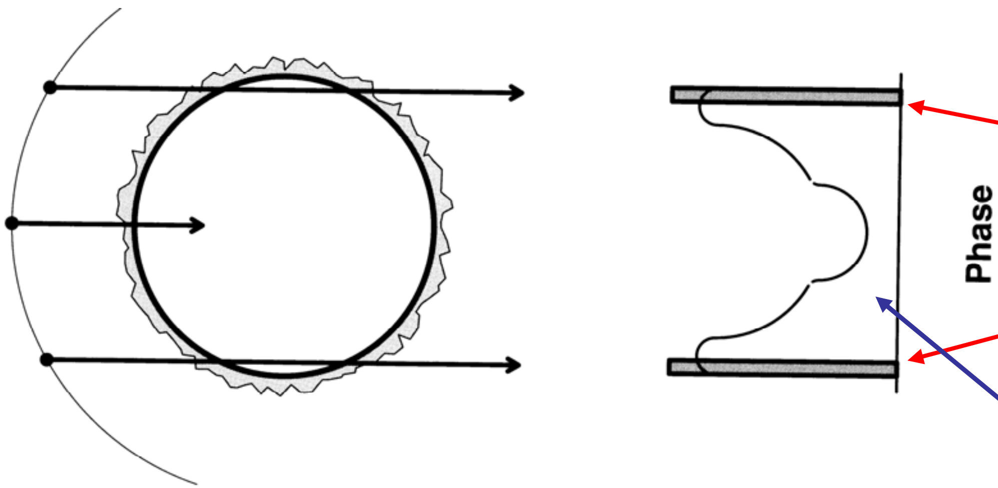

Fig. 10.3. The Vestrand–Eichler model of signal production in a binary system and the light curve for γ-ray (shaded) and neutrino fluxes.

Neutrini cosmici da AGN

Alla produzione di fotoni attraverso il meccanismo SSC (Synchrotron-Self-Compton) si somma la produzione attraverso il meccanismo adronico → fotoni di energie piu' elevate e neutrini

π carichi prodotti in reazioni di fotoproduzione:

$p + \gamma \rightarrow p(n) + m\,\pi^{+/-} + n\,\pi^0$

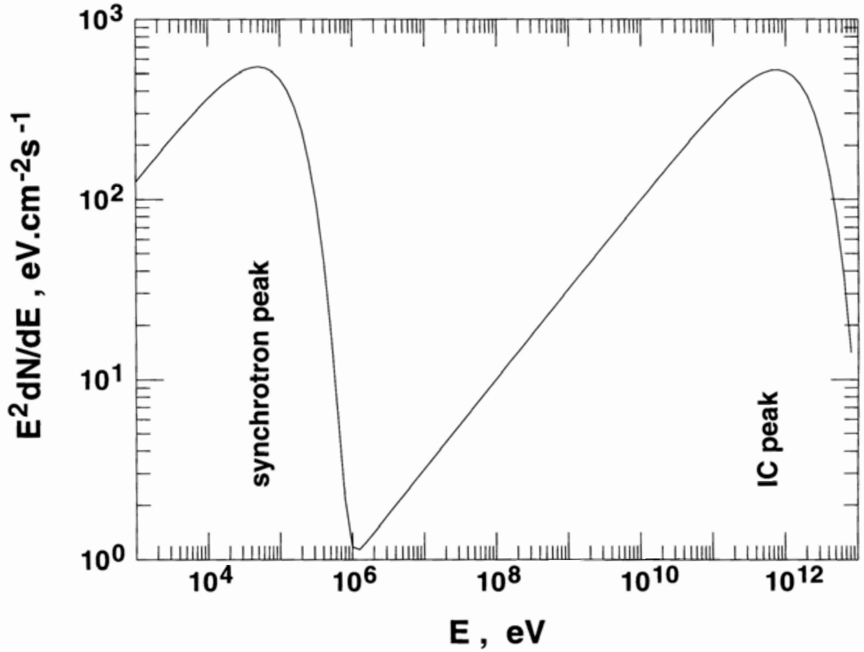

Fig. 10.9. Two-peaked photon spectrum generated by the Synchrotron Self Compton model of γ-ray production.

Neutrini cosmici predetti da sorgenti note

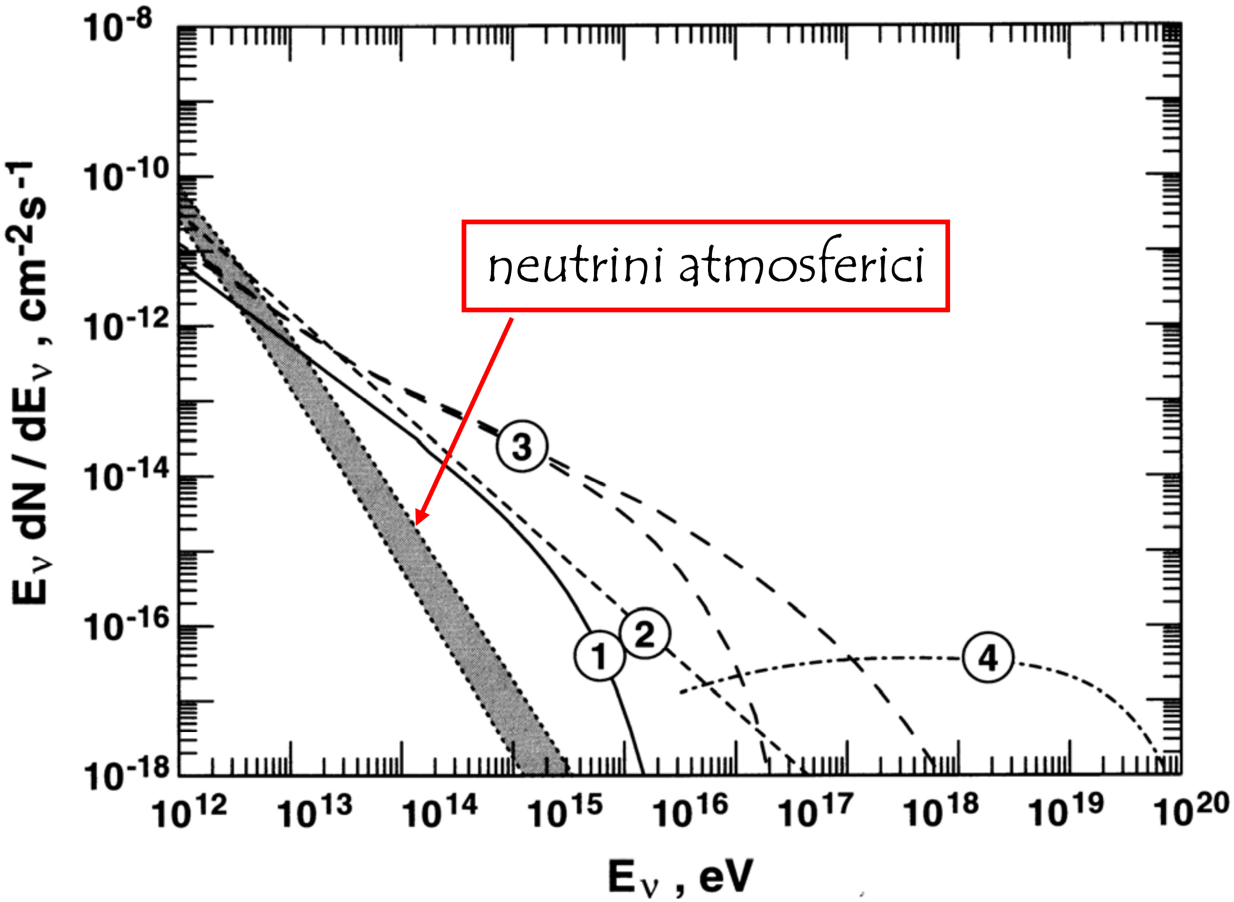

Fig. 10.12. Predictions of neutrino fluxes from different types of sources. (1) is the neutrino flux that would correspond to the gamma-rays of SNR IC443. (2) is the neutrino emission that would correspond to hadronic origin of the Mrk 501 gamma-ray outburst. (3) is the range of neutrino emission from the core of 3C273, and 4) is a prediction for the neutrino emission of 3C279. The shaded are shows the atmospheric neutrino flux within 1° – from high (horizontal) to vertical.

Neutrini cosmici diffusi

Fondo da neutrini prodotti in interazioni dei raggi cosmici nell'atmosfera: spettro molto piu' ripido (concentrato a basse energie)

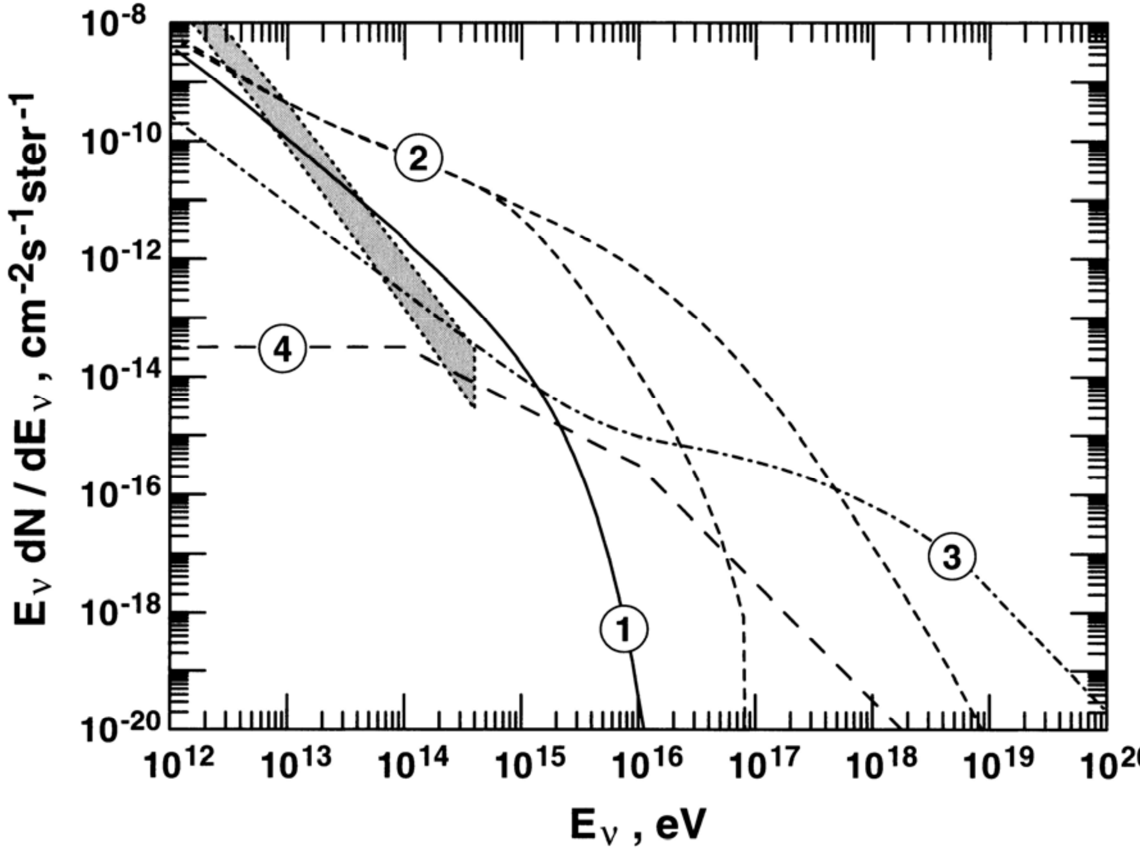

Fig. 10.13. Predictions for diffuse neutrino fluxes. The shaded area shows the horizontal (higher) and vertical fluxes of atmospheric neutrinos. Curve (1) is for the central region of the Galaxy, (2) corresponds to the curves (3) from Fig. 10.12, (3) is the prediction of Ref. [359] and (4) is the prediction of the GRB neutrinos of Ref. [358].

Rivelatori

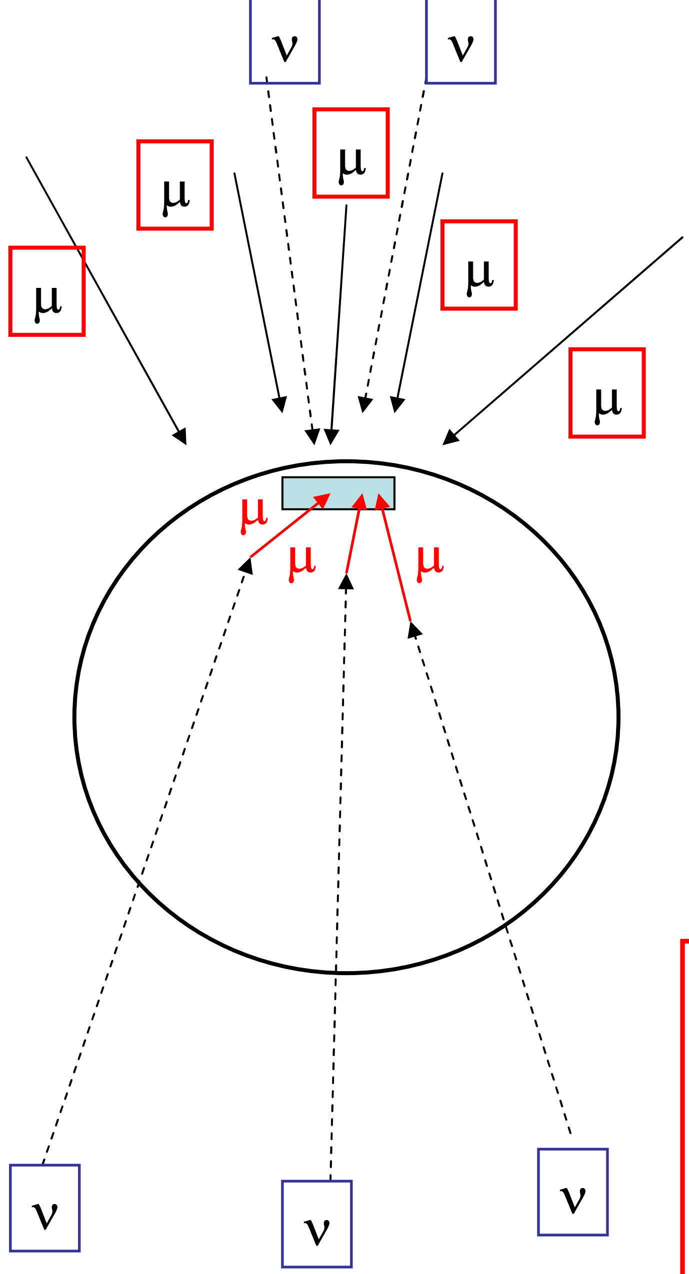

Rivelatori posti nell'emisfero Nord "guardano" verso il basso

Rivelatori posti nell'emisfero Sud "guardano" verso l'alto

Reazioni utilizzabili :

$$\nu_\mu + N \rightarrow \mu^- + adroni \quad (p, n, \pi^\pm, \pi^0, K^\pm, K^0 ....)$$

$$\bar{\nu}_\mu + N \rightarrow \mu^+ + adroni$$

Il mesone μ prodotto nell'interazione del <u>neutrino</u> ha circa meta' dell'energia di questo. Ad energie molto elevate viaggia nella medesima direzione del neutrino.

Rivelatori

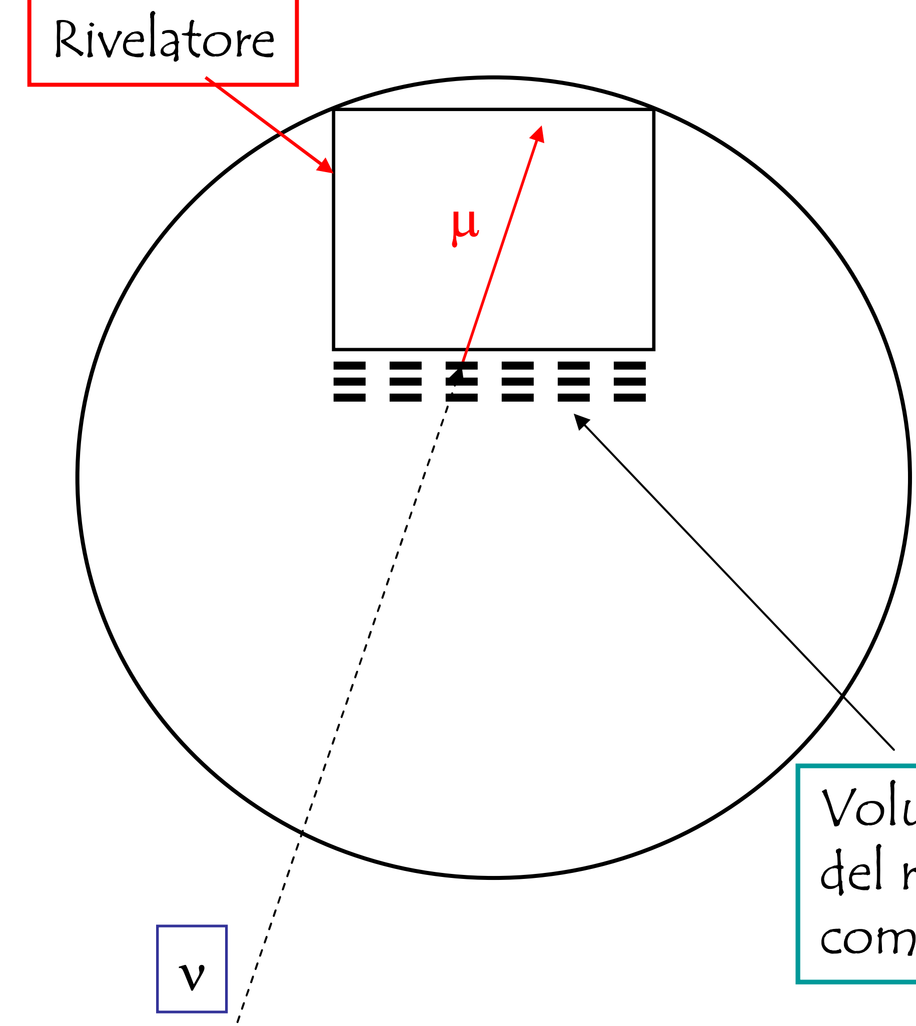

Reazioni utilizzabili :

$$\nu_\mu + N \to \mu^- + adroni \quad \left(p, n, \pi^\pm, \pi^0, K^\pm, K^0 ....\right)$$

$$\bar{\nu}_\mu + N \to \mu^+ + adroni$$

Direzione ed energia del mesone μ misurate attraverso la rivelazione della luce Cerenkov emessa in acqua

Volume utile molto maggiore del volume del rivelatore (utilizzo della roccia sottostante come "bersaglio")

Neutrinos weakly interacting in matter

Low cross-section
good :
Astronomic sources and universe transparent to neutrinos

Earth transparent up to 100 TeV

bad:
Need massive detector

Interaction length of neutrinos vs energy

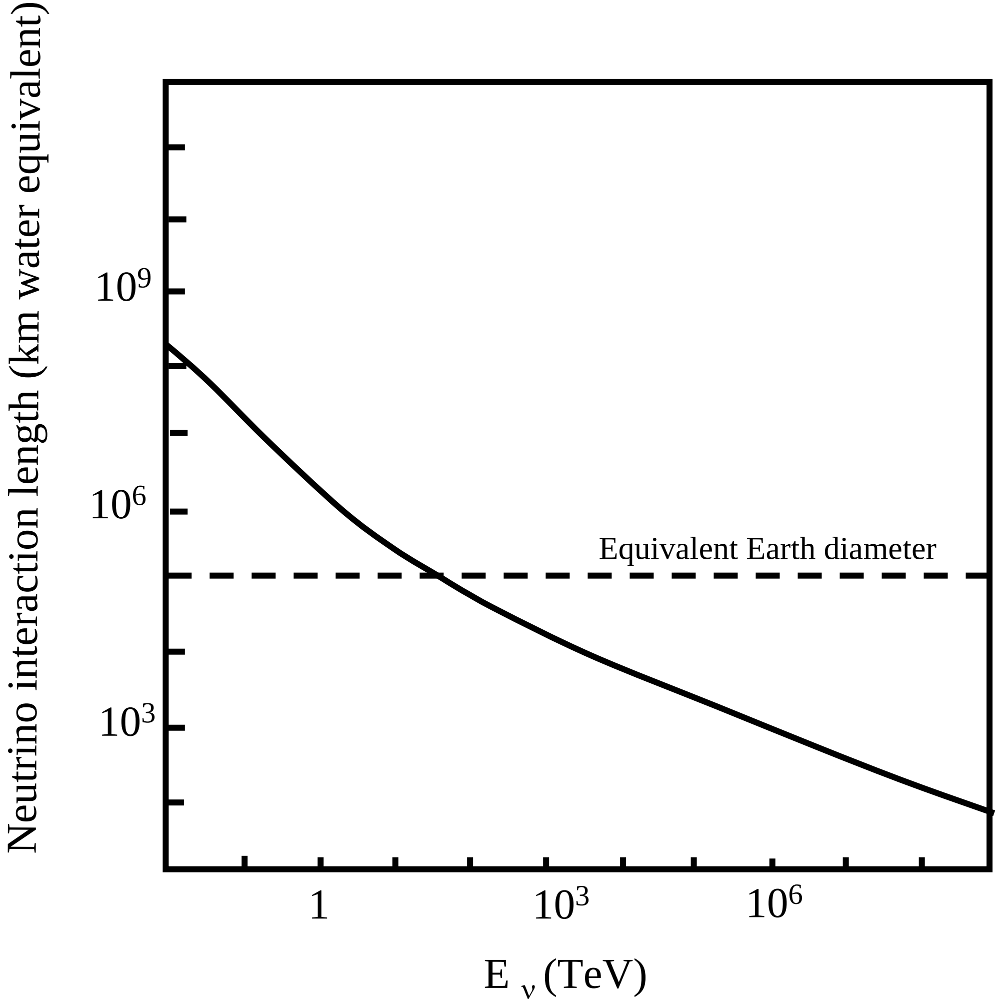

Neutrino Interactions in water/earth

3 flavours of neutrino, 2 types of interaction: 4 topologies of light production in water

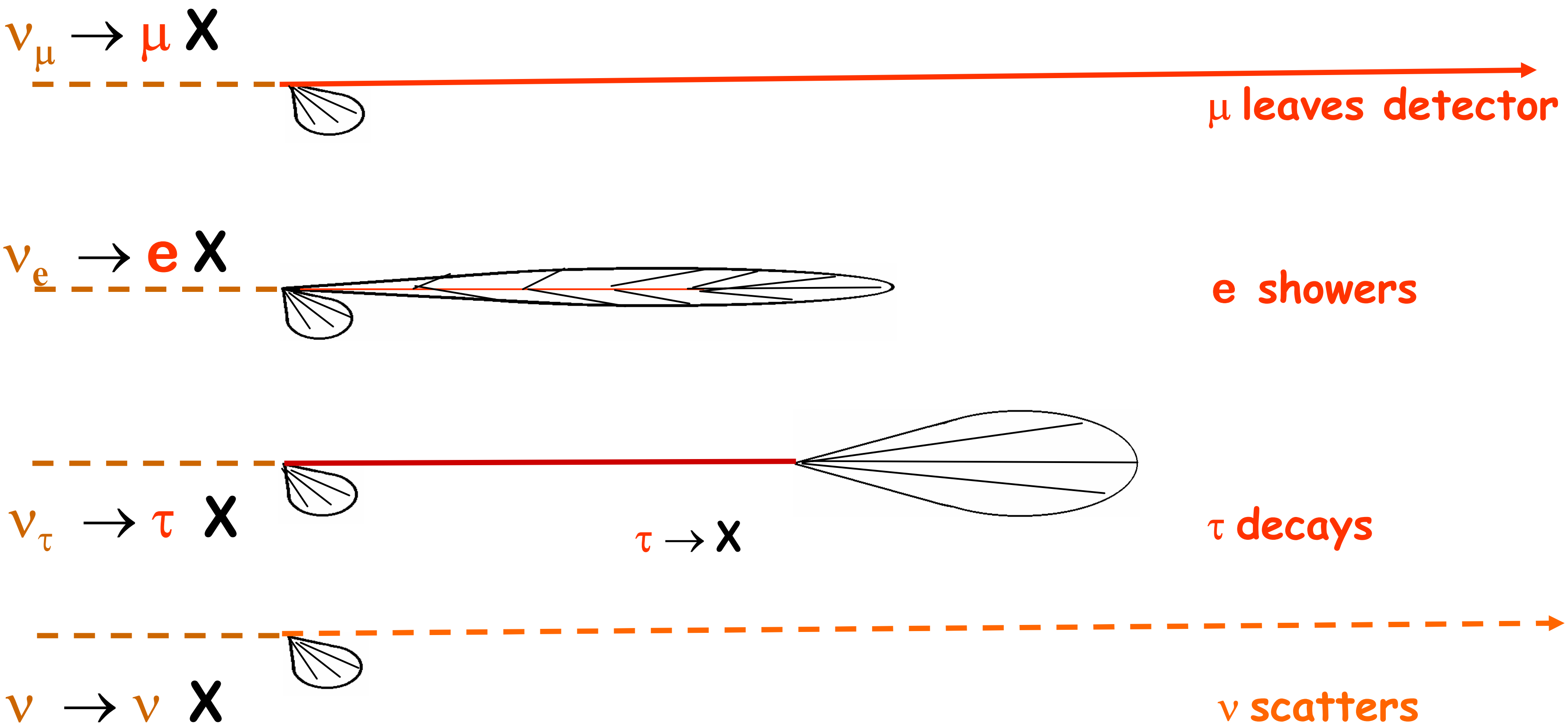

Detectors optimised for $\nu_\mu \rightarrow \mu$ **X,** other modes have lower detection efficiency

Neutrino Telescope Projects

ANTARES La-Seyne-sur-Mer, France
(NEMO Catania, Italy)

BAIKAL: Lake Baikal, Siberia

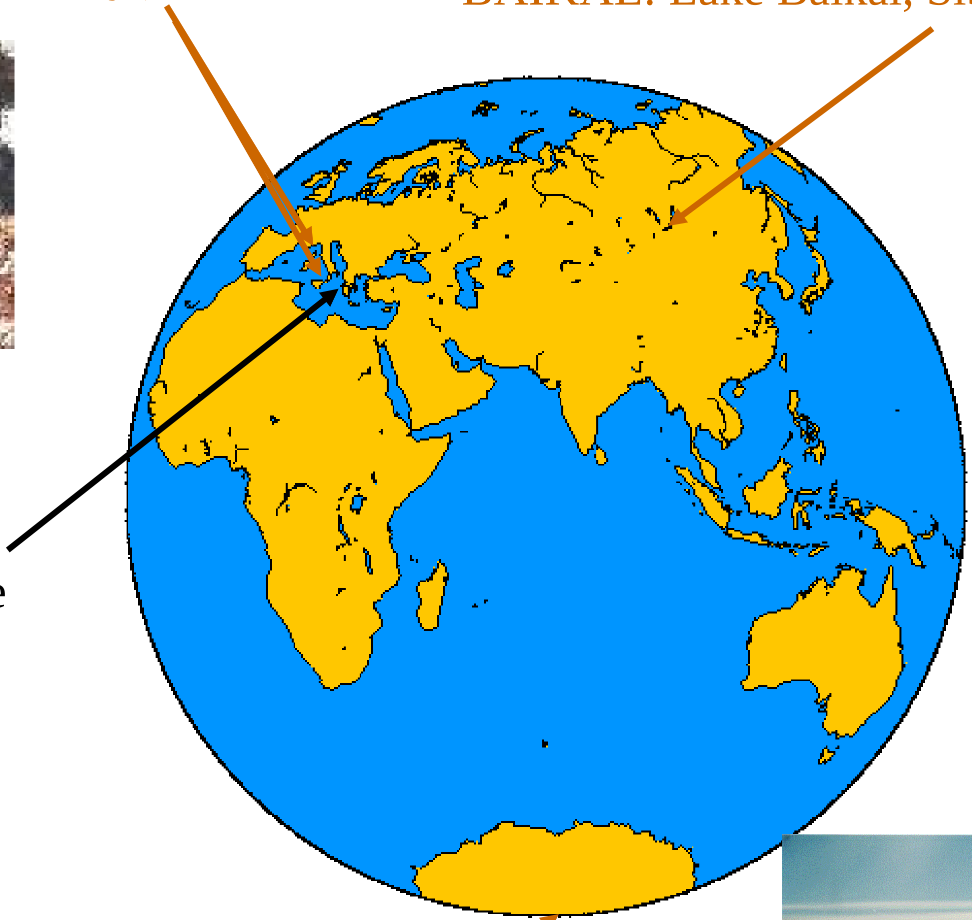

NESTOR : Pylos, Greece

AMANDA, South Pole, Antarctica

Principle of H_2O Cherenkov Neutrino Astronomy

Muon track direction from arrival time of light

Neutrino direction: $\Delta(\theta_\nu - \theta_\mu) \approx 0.7^o / E^{0.6}(TeV)$

Muon energy from energy loss and range

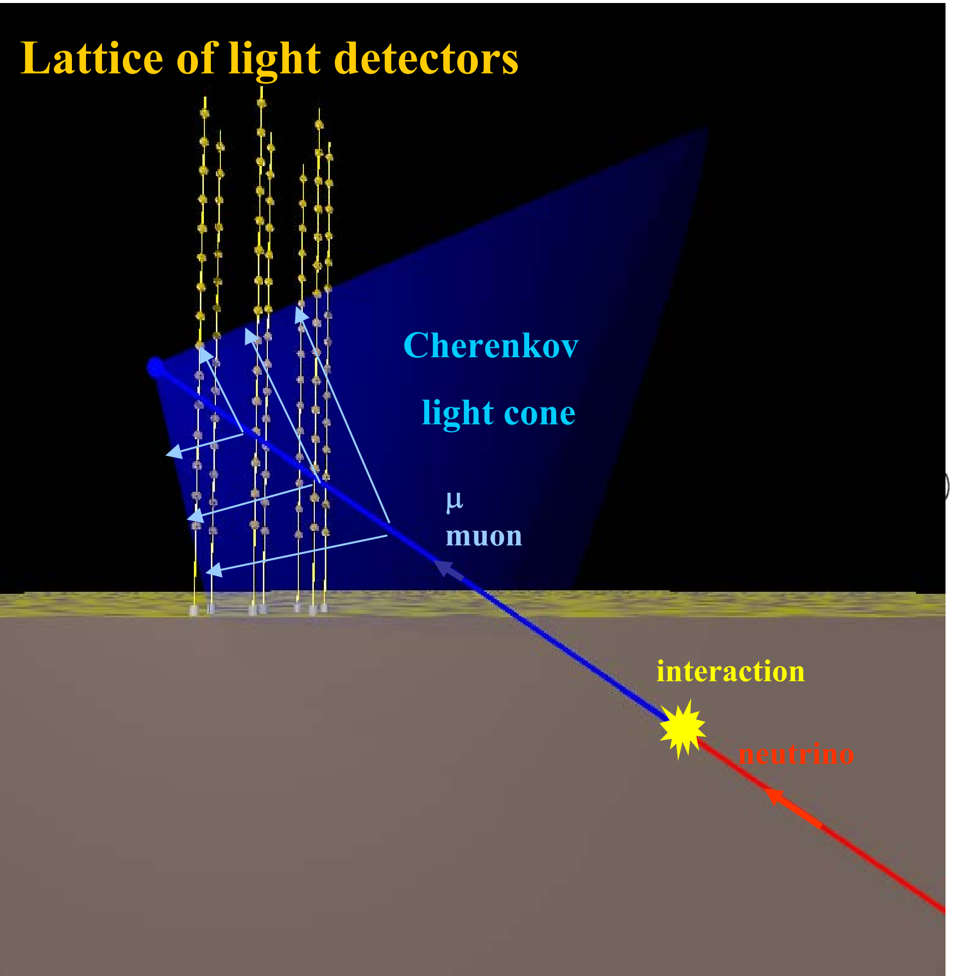

Sky map of origins of neutrinos
(Galactic co-ordinate system)

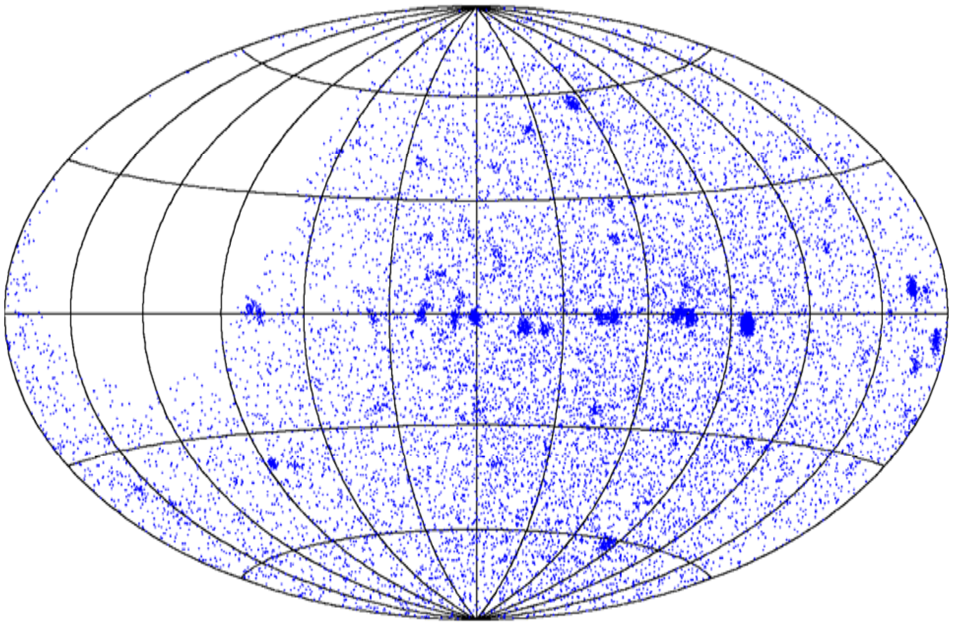

Baikal

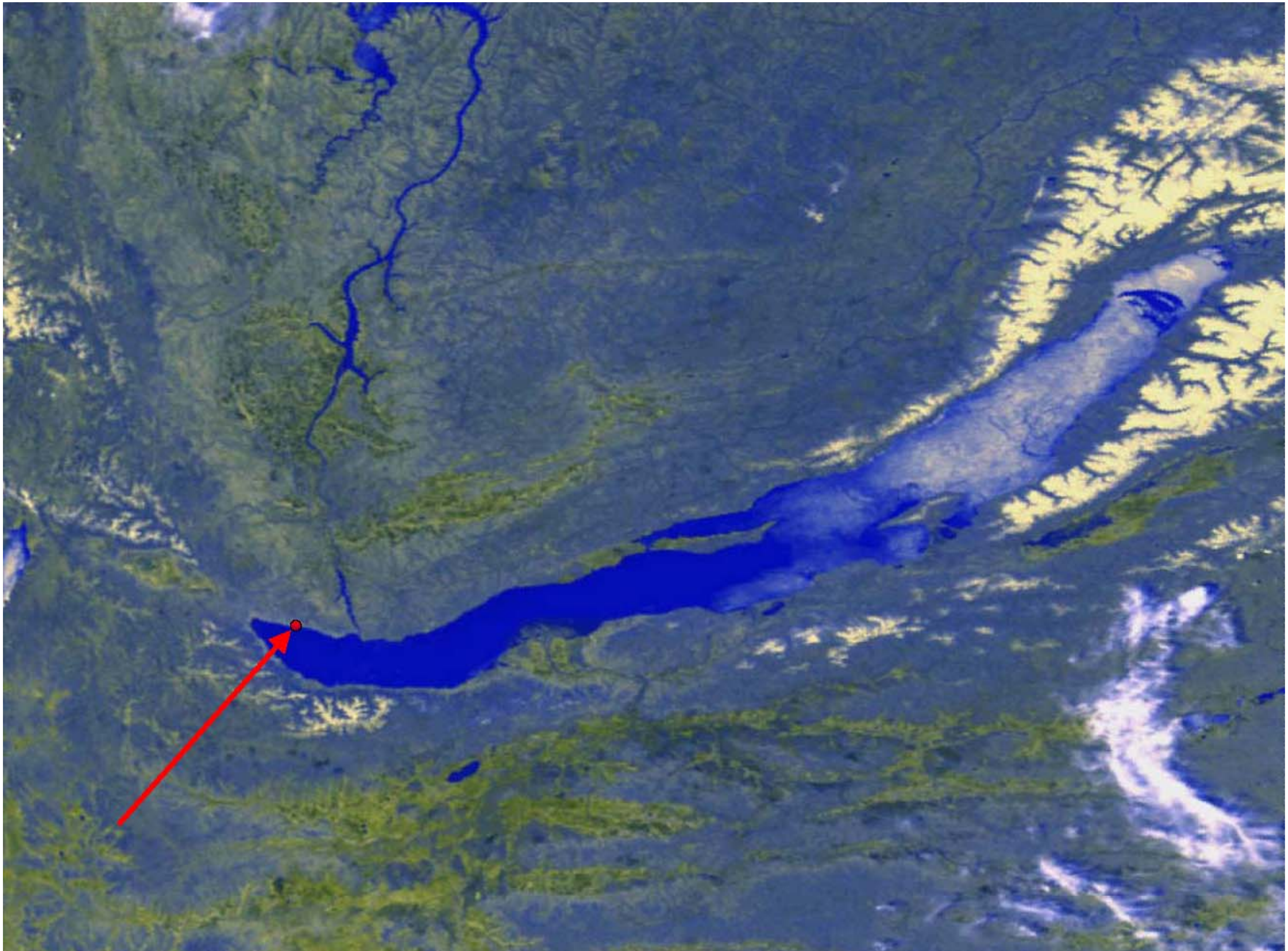

Baikal

The Site

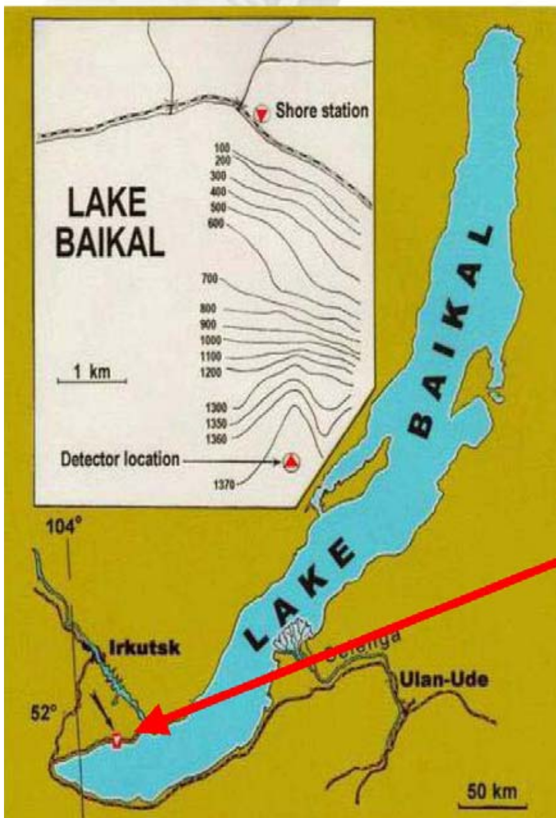

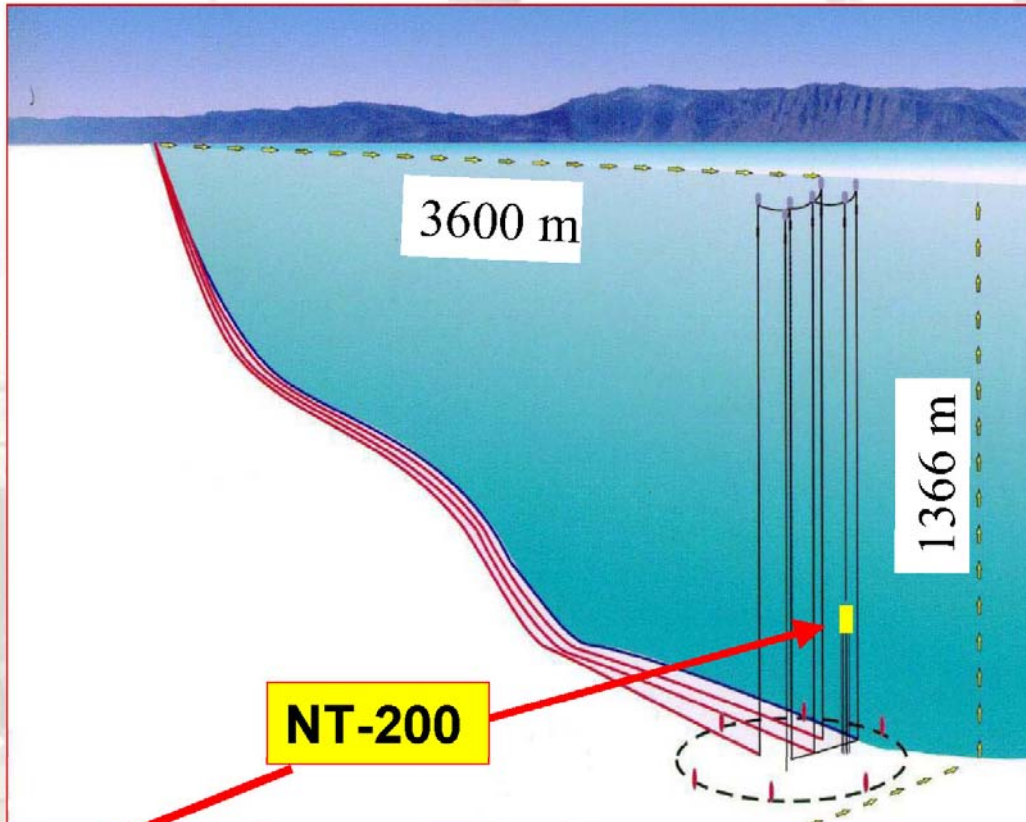

- 4 cables x 4km to shore.
- 1070m depth

Ice – A perfect natural deployment platform

March, 2005, 4km off-shore:
NT200+ deployment from ice.

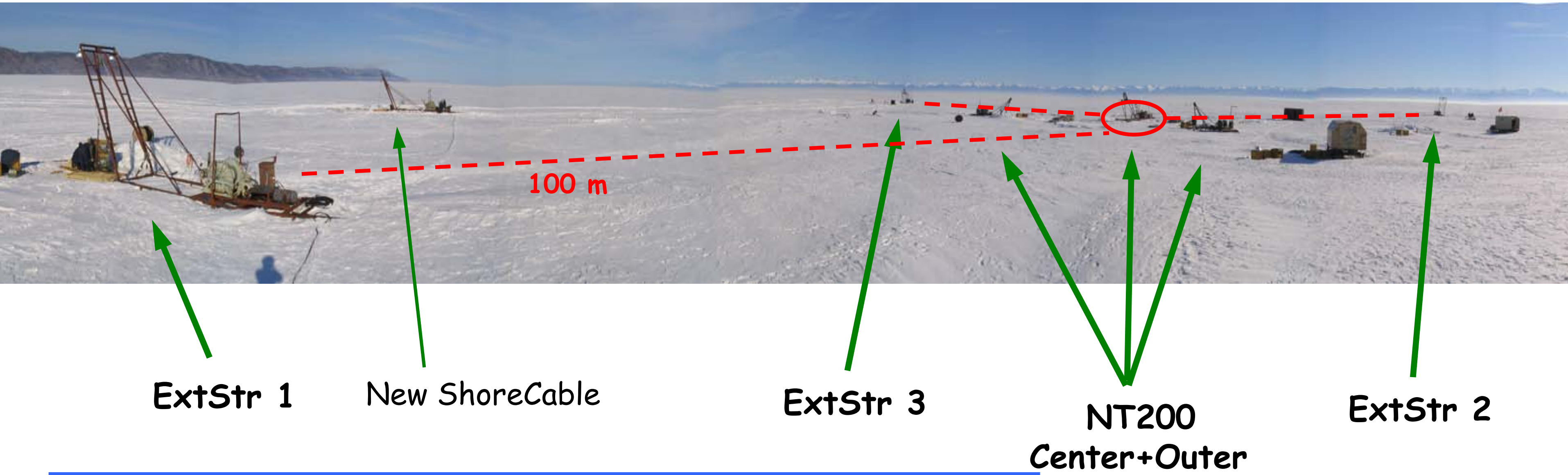

- Ice is stable for 6-8 winter-weeks/year:
  - Upgrades & maintenance
  - Test & installation of new equipment
  - Operation of surface detectors (EAS, acoustics,…)
  - Electrical winches used for deployment operations

Baikal - Optical Properties

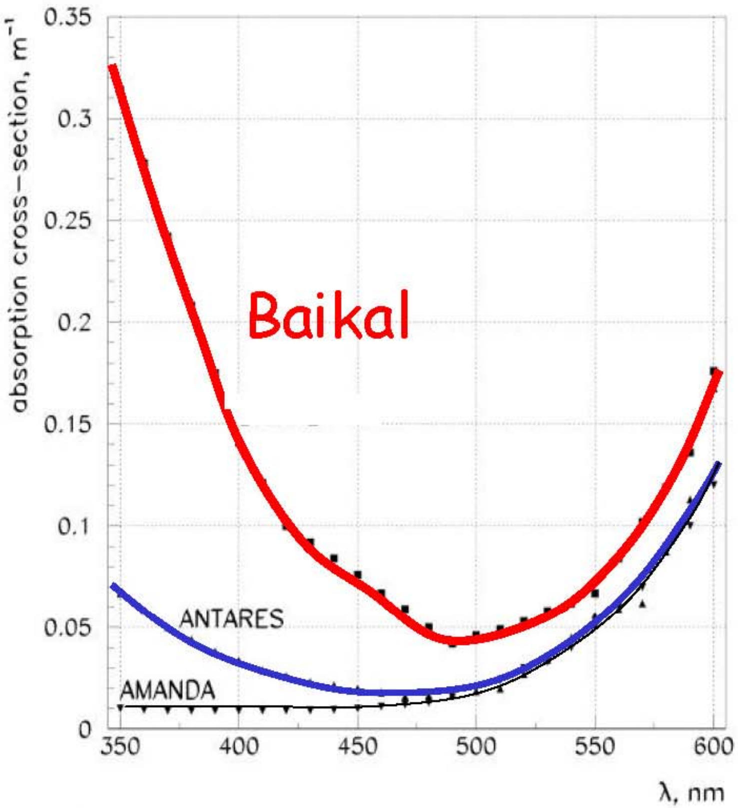

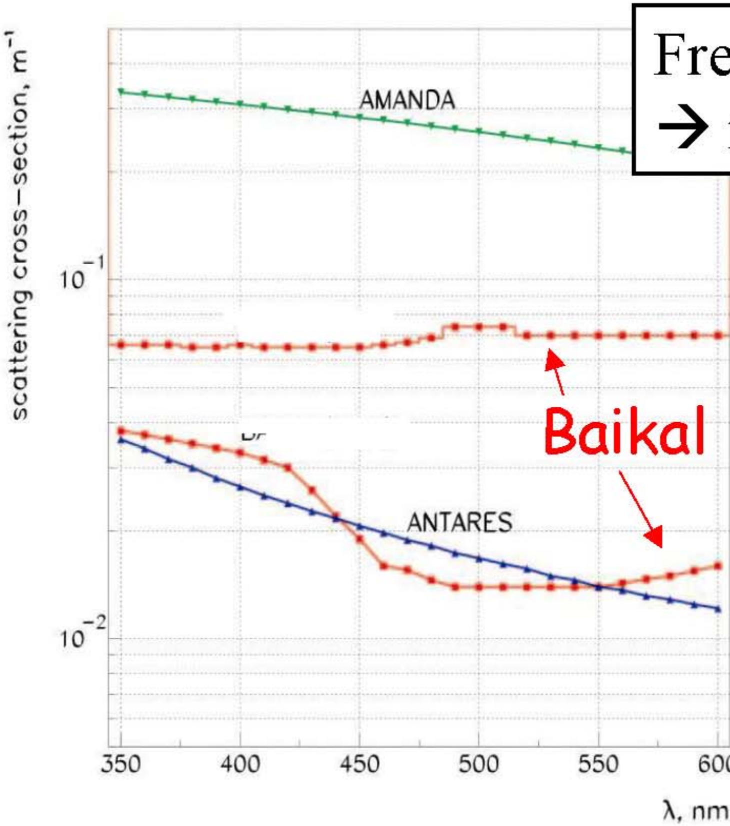

FreshWater
→ no K40 BG

Abs. Length: 22 ± 2 m

In-situ measurements

Scatt. Length (geom) ~ 30-50 m
⟨cos Θ⟩ ~ 0.85-0.9

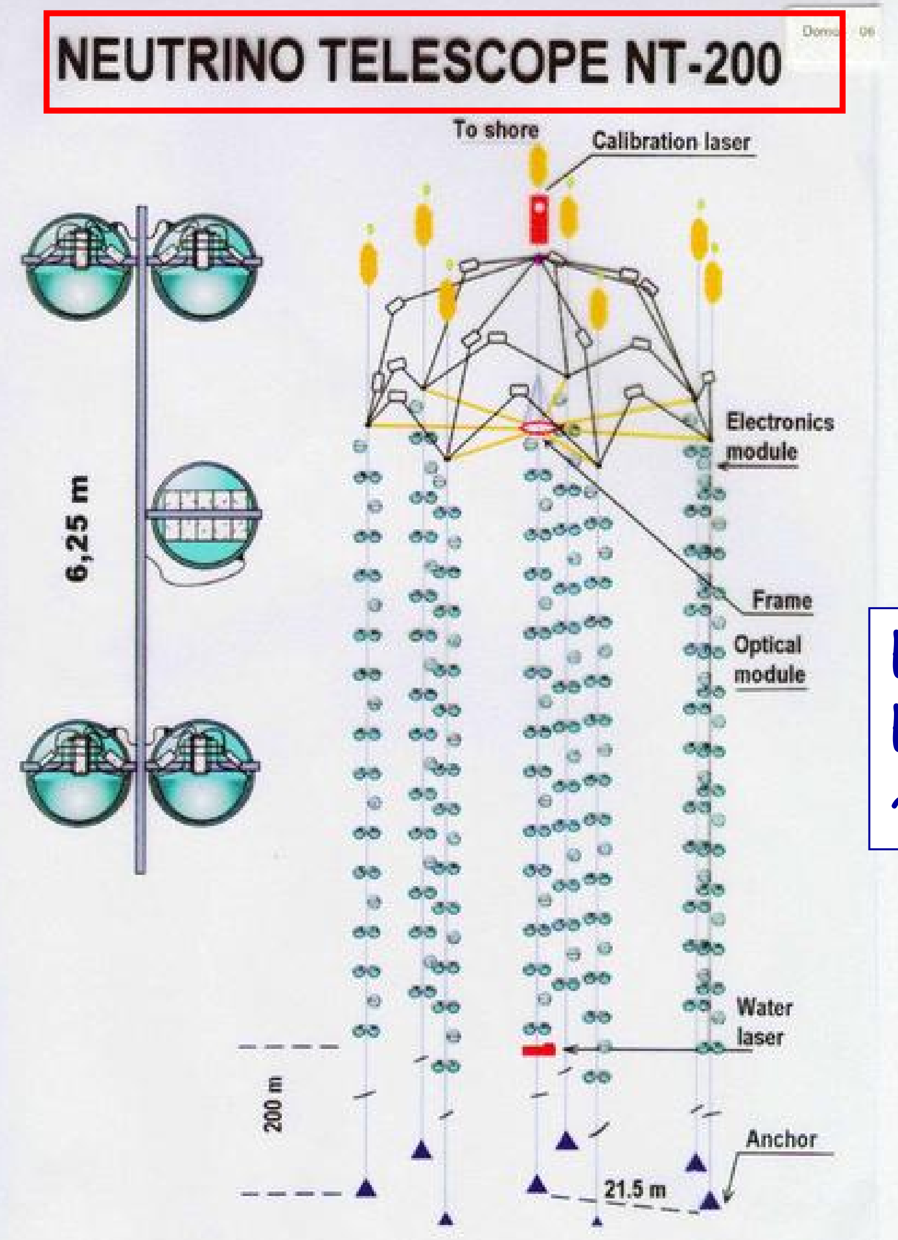

- 8 strings: 72m height
- 192 optical modules
  = 96 pairs (coincidence)
- measure T, Charge
  - σ_T ~ 1 ns
  - dyn. range ~ 1000 p.e.

Effective area: 1 TeV ~2000 m^2
Eff. shower volume: 10TeV ~0.2Mt

Height × ∅ = 70m × 40m, $V_{geo}=10^5 m^3$

Quasar PM: d=37cm

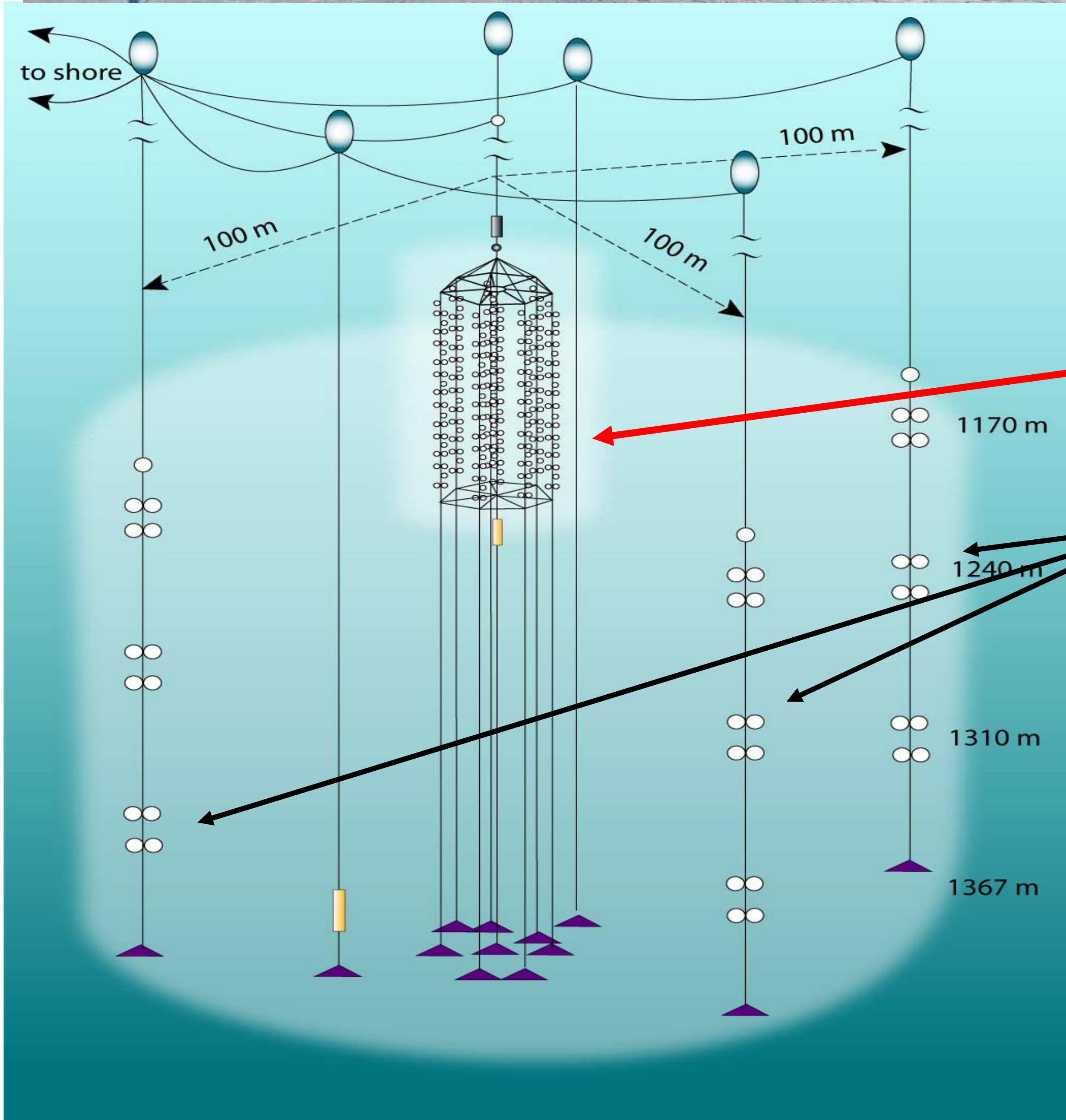

NT200+ = NT200 + 3 long outer strings

- **Height = 210m**
- **∅ = 200m**
- **Volume ~ 5 Mton**

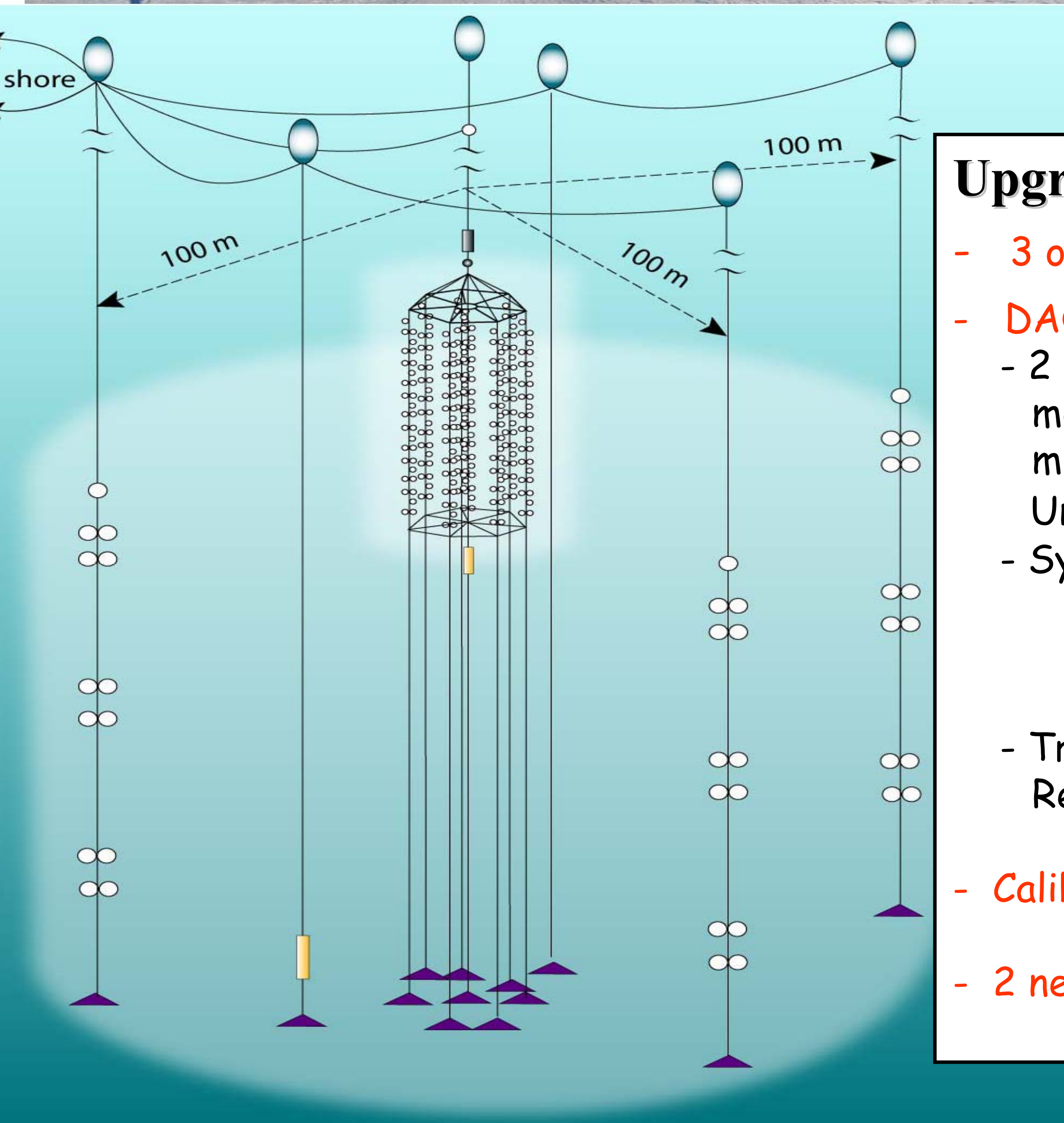

Upgrade 2003-2005:

- 3 outer strings were installed
- DAQ – modernization
  - 2 Underwater PC with Flex DSL modem (1 Mbps), full multiplexing, Underwater Ethernet
  - Synchronization unit
    * time synchronization (~ ns) NT200 <-> outer strings
    * event building
  - Transition to Linux, RemoteCntrl.
- Calibration - New bright Laser
- 2 new cables to shore (2x4 km)

Eventi ν in Baikal

Search for High Energy - Cascades

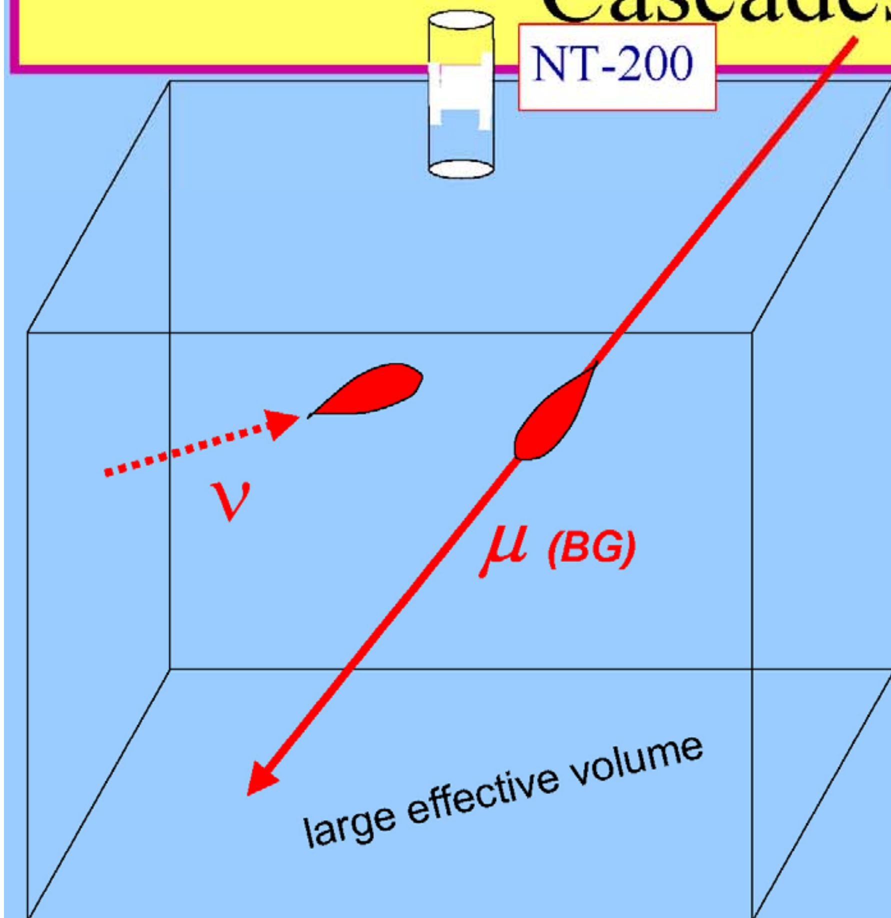

Look for upward moving light fronts.

<u>Signal:</u>
isolated cascades from neutrino interactions

<u>Background:</u>
Bremsshowers from h.e. downward muons

Final rejection of background by „energy cut" ($N_{channel}$)

Un evento di neutrino in Baikal

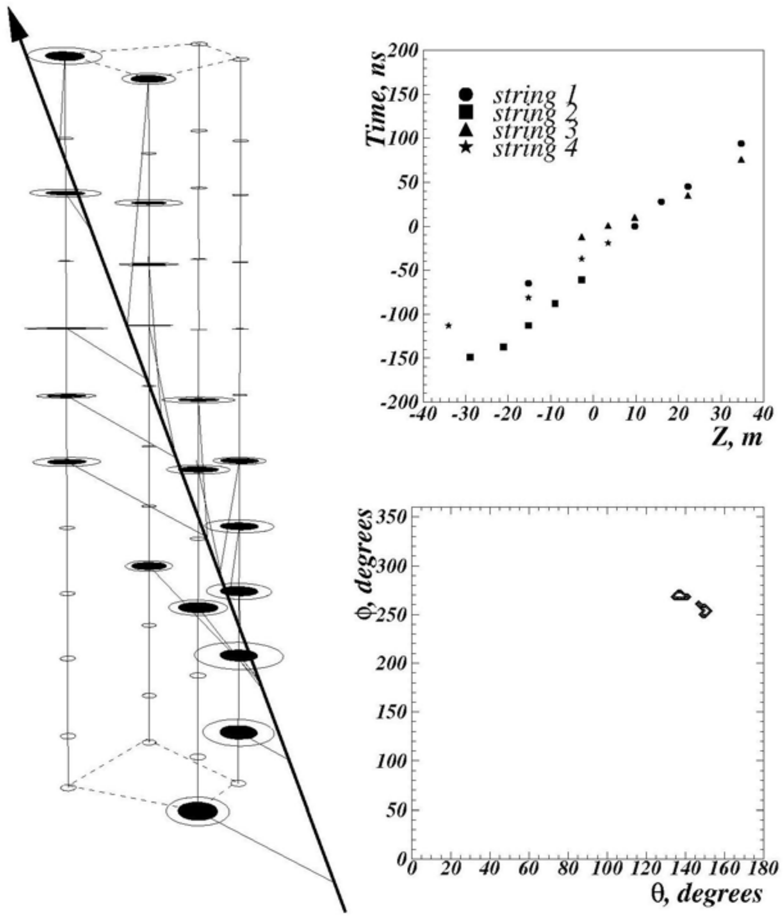

Figure 3: A "gold plated" 19-hit neutrino event. *Left:* Event display. Hit channels are in black. The thick line gives the reconstructed muon path, thin lines pointing to the channels mark the path of the Cherenkov photons as given by the fit to the measured times. The sizes of the ellipses are proportional to the recorded amplitudes. *Top right:* Hit times versus vertical channel positions. *Bottom right:* The allowed θ/ϕ regions (see text).

Atmospheric Muon-Neutrinos

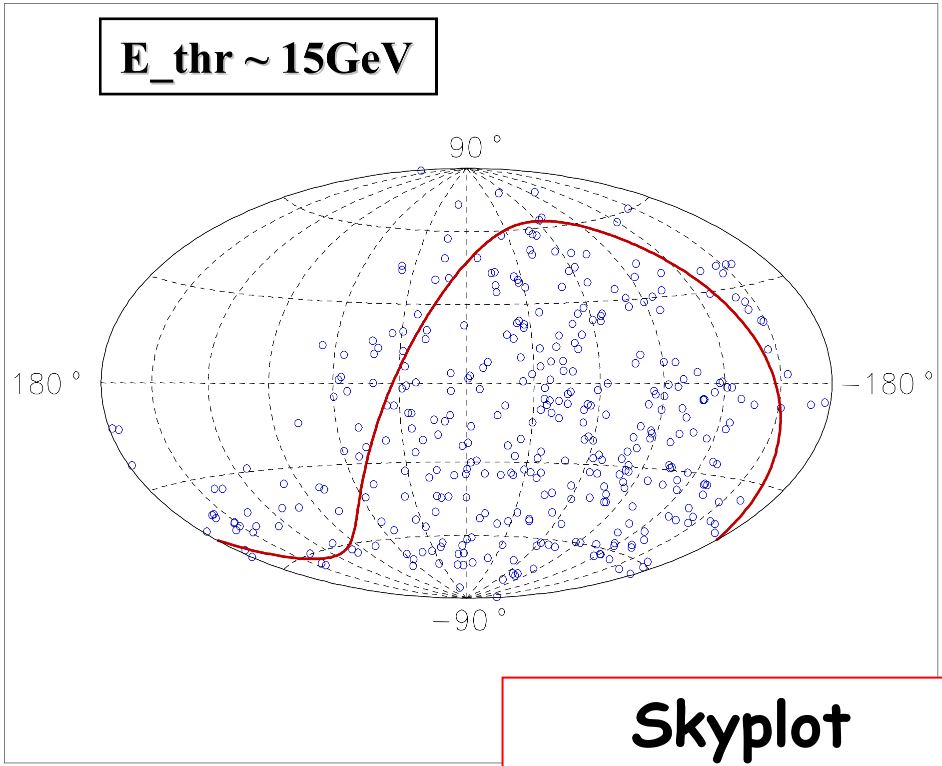

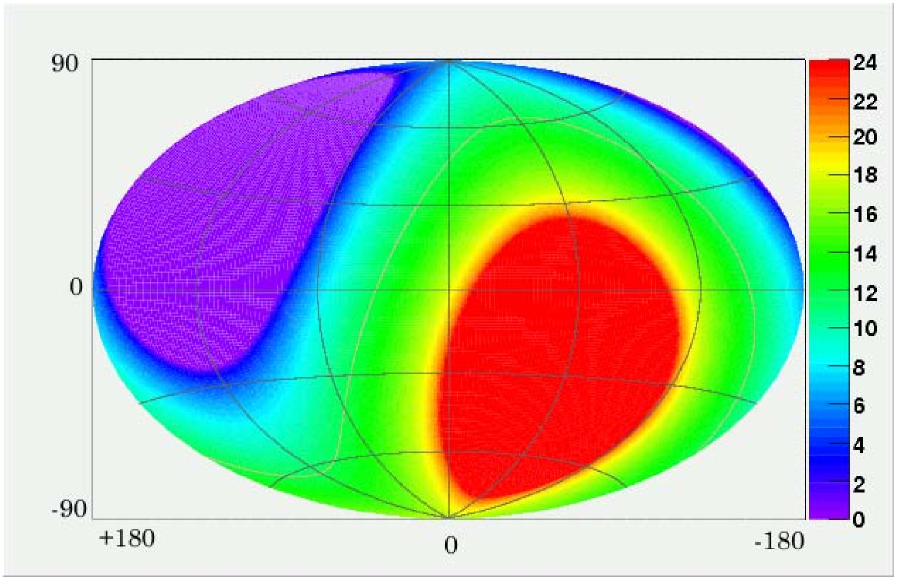

Skyplot
(galactic coordinates)

- With looser cuts, 1998-2002: 372 events. N_μ(>15GeV)/N_μ(>1GeV)~1/7
  → A higher statistics neutrino sample for Point-Source Search.
- MC: 385 ev. Expected (15%BG).

Search for High Energy Cascades

NT-200 is used to watch the volume below for cascades.

Look for upward moving light fronts.

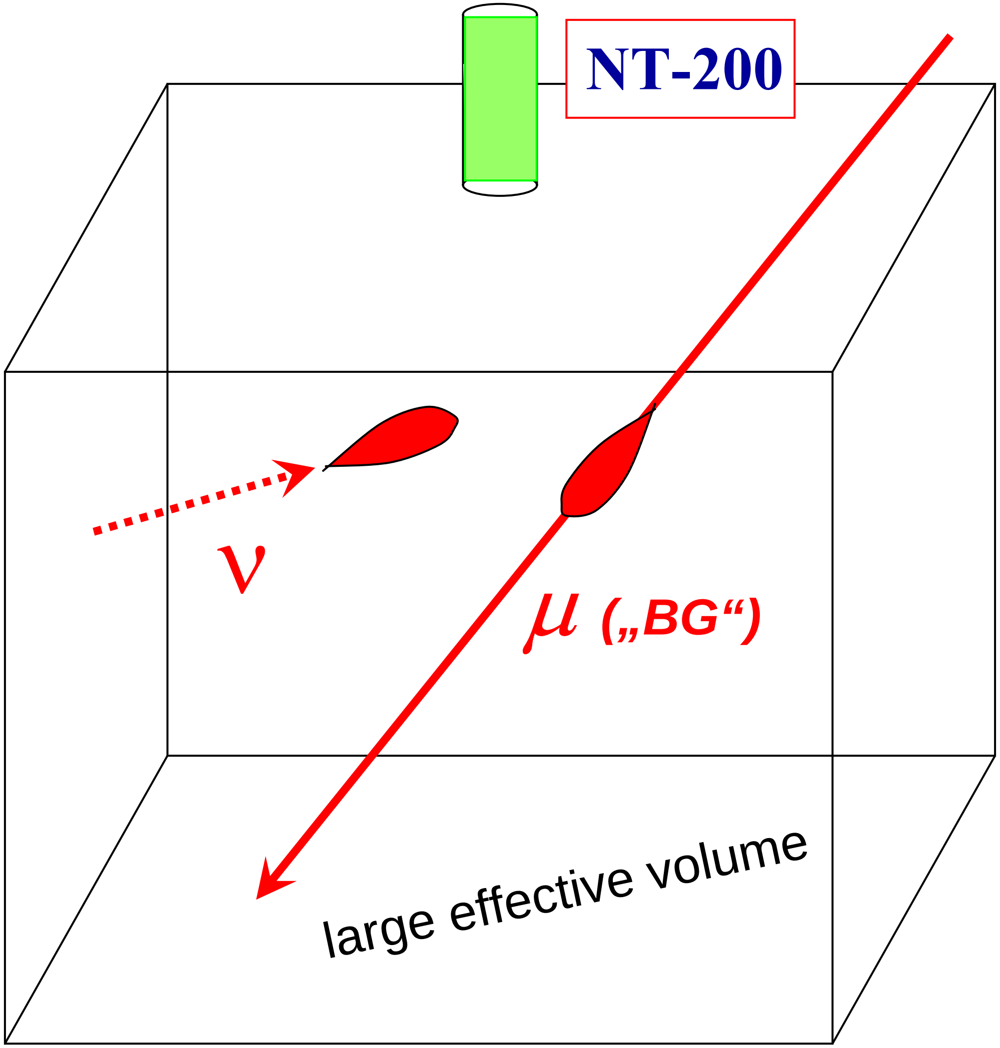

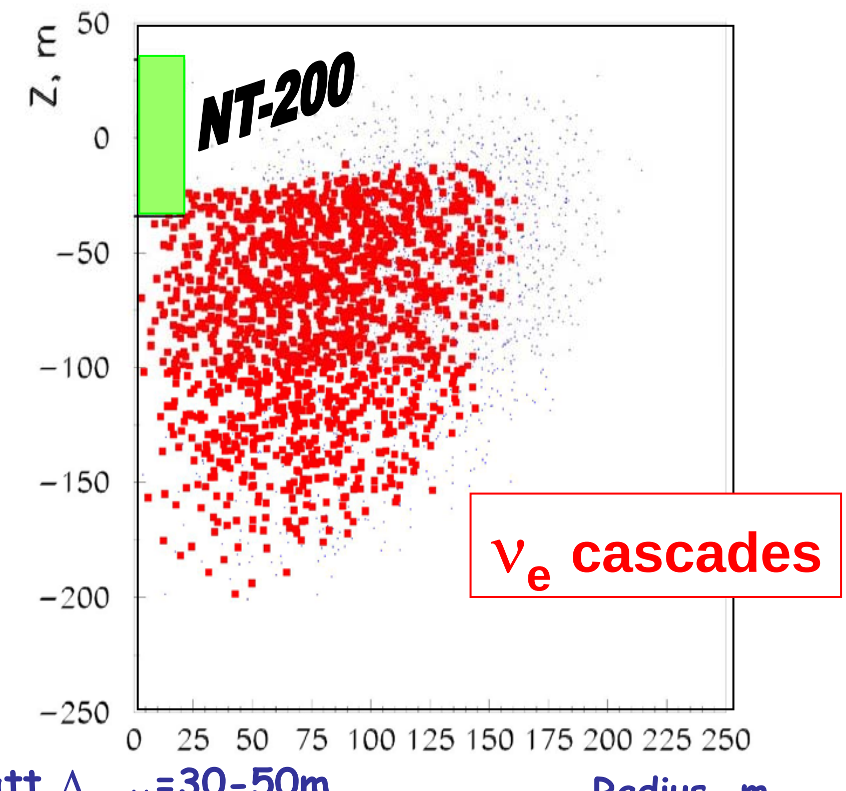

Allowed by excellent scatt Λ_{scatt}=30-50m

Search for High Energy Cascades

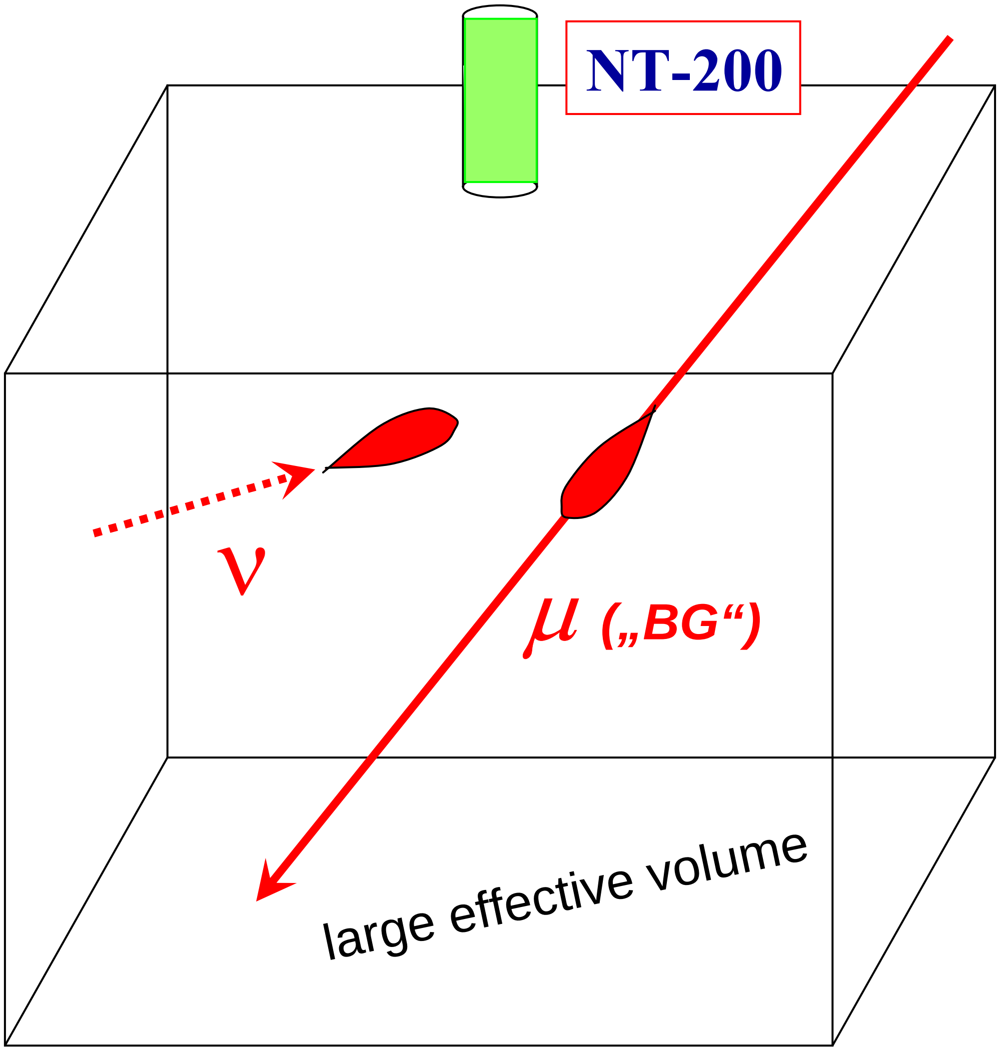

NT-200 is used to watch the volume below for cascades.

Physics topics:

- HE cascades from
  ν_e ν_μ ν_τ - NC/CC
  - ❑ Diffuse astroph.flux
  - ❑ GRB correlated flux
- HE atmospheric muons
  (the „BG“ to ν's)
  - ❑ Prompt μ
  - ❑ Exotic μ
- ...

Selezione di eventi di alta energia

<u>Hard signal spectra would pile up</u> in the "energy parameter"

N_{hit} = Number of Channels hit

Shape of signal in N_{hit} distribution for $\Phi_\nu = A\,E^{-\gamma}$ (γ=1.5, 2.0, 2.5).

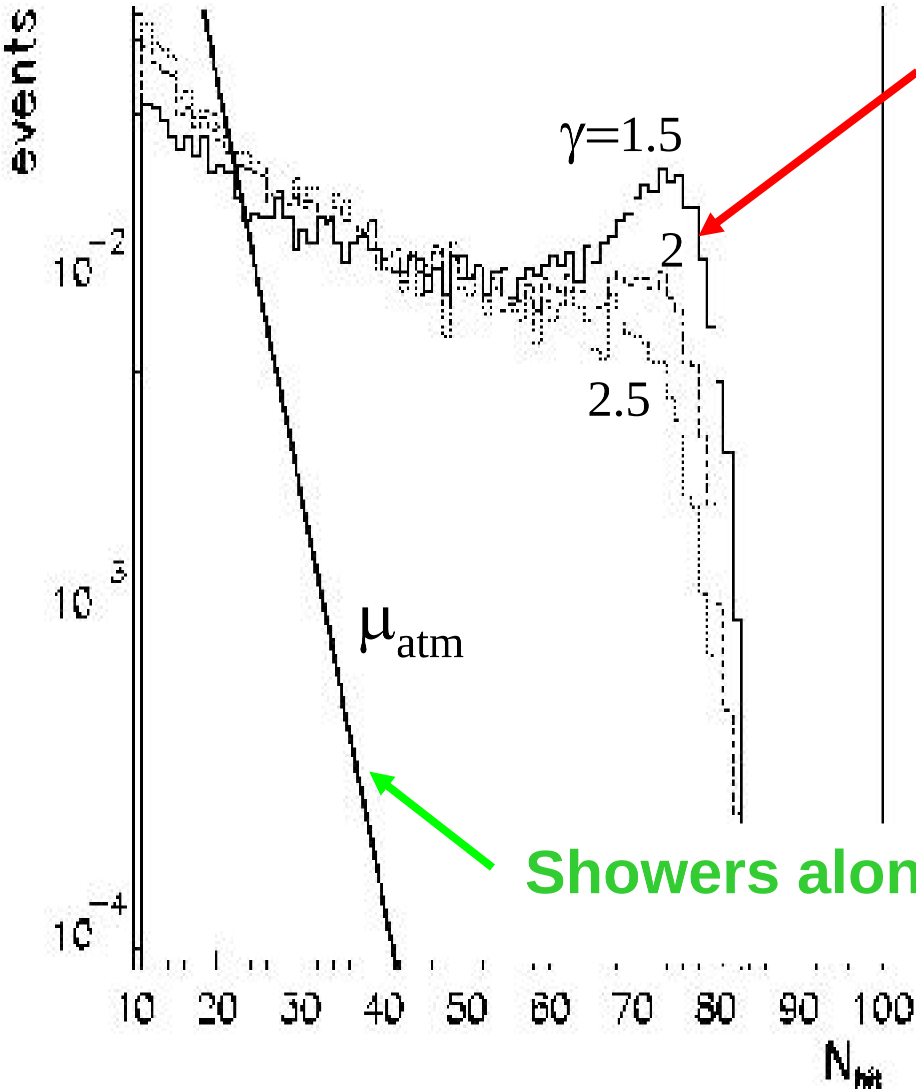

Showers along $\mu_\downarrow$

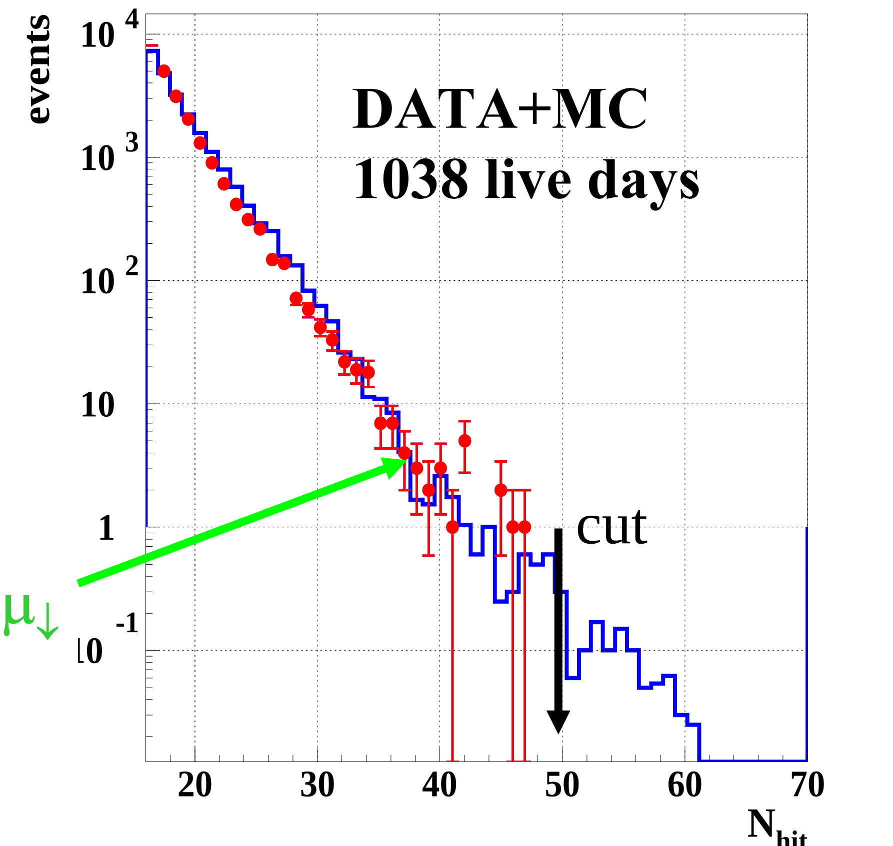

Diffuse Flux ν_e, ν_τ, ν_μ Limit

Effective Volume vs. Energy

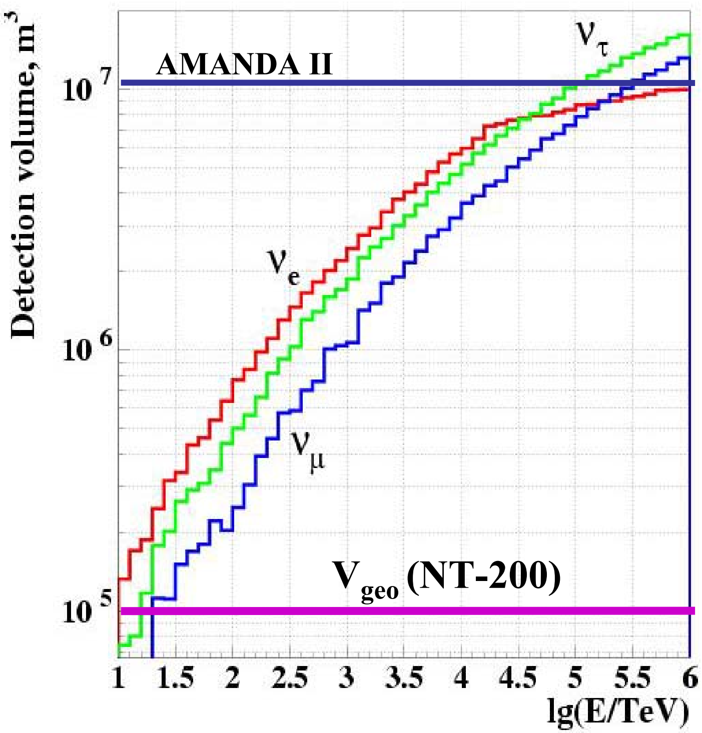

V_{eff} > 1 Mton at 1 PeV

No events observed (+ 24% system. err.) **→ 2.5 evt exp.**

The 90% C.L. "all flavour" limit (1038 days)
for a γ=2 spectrum $\Phi_\nu \sim E^{-2}$ (20 TeV < E < 50 PeV),

and assuming $\nu_e:\nu_\mu:\nu_\tau$ = 1 : 1 : 1 at Earth (1 : 2 : 0 at source)

$$E^2 \Phi_\nu < 8.1 \cdot 10^{-7} \text{ GeV cm}^{-2} \text{ s}^{-1} \text{ sr}^{-1}$$ (Baikal 2005)

$$E^2 \Phi_\nu < 8.6 \cdot 10^{-7} \text{ GeV cm}^{-2} \text{ s}^{-1} \text{ sr}^{-1}$$ (Cascades AMANDA-II, 2004)

90% C.L. Limit via W-RESONANCE production
(E = 6.3 PeV, $\sigma = 5.3 \cdot 10^{-31}$ cm^2)

$$\Phi_{\nu e} < 3.3 \cdot 10^{-20} (\text{cm}^2 \cdot \text{s} \cdot \text{sr} \cdot \text{GeV})^{-1}$$ (Baikal 2005)

$$\Phi_{\nu e} < 5.0 \cdot 10^{-20} (\text{cm}^2 \cdot \text{s} \cdot \text{sr} \cdot \text{GeV})^{-1}$$ (AMANDA 2004)

Amanda

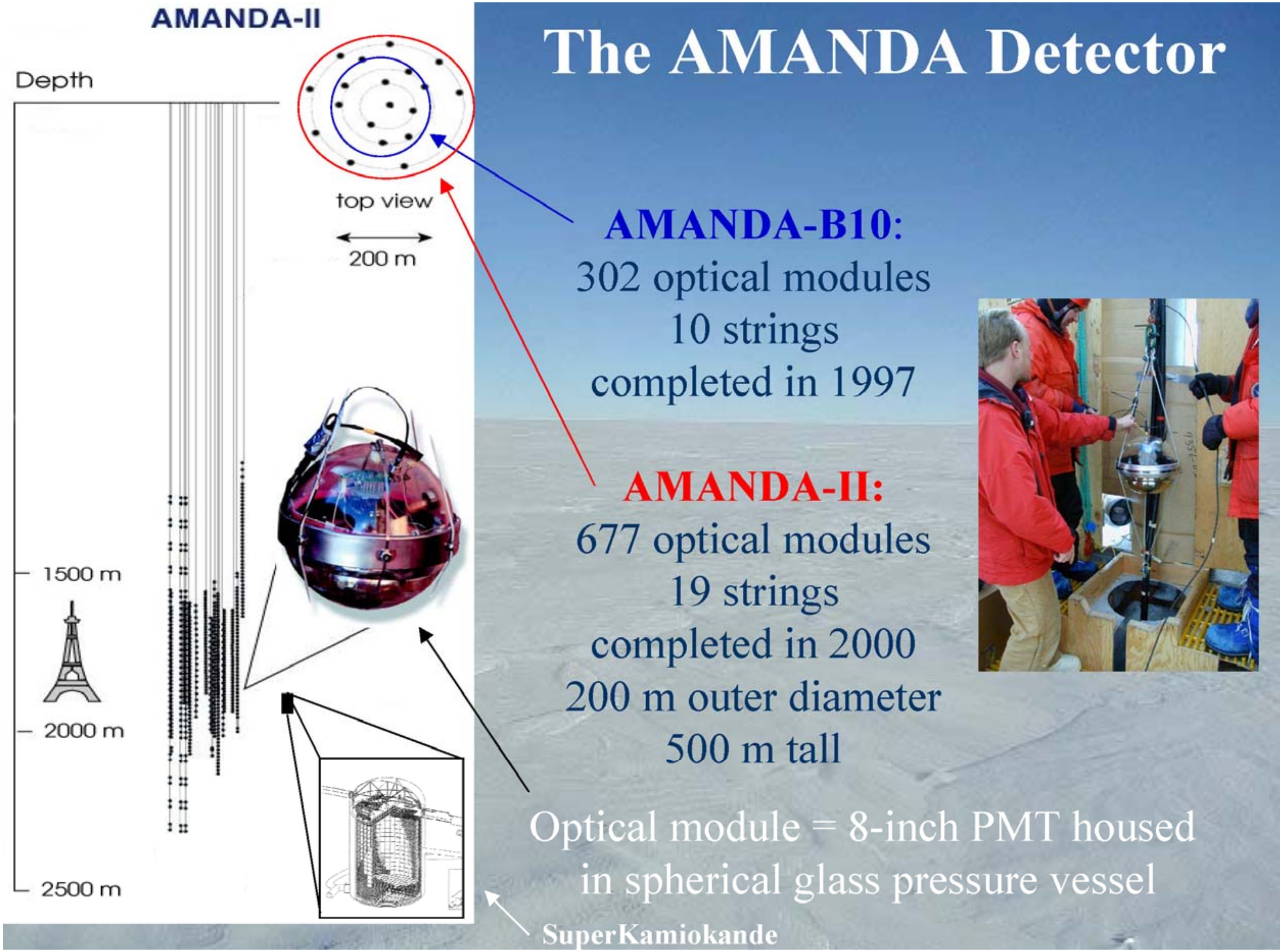
AMANDA-II
Depth
top view
200 m
1500 m
2000 m
2500 m
The AMANDA Detector
AMANDA-B10:
302 optical modules
10 strings
completed in 1997
AMANDA-II:
677 optical modules
19 strings
completed in 2000
200 m outer diameter
500 m tall
Optical module = 8-inch PMT housed
in spherical glass pressure vessel
SuperKamiokande

Amanda

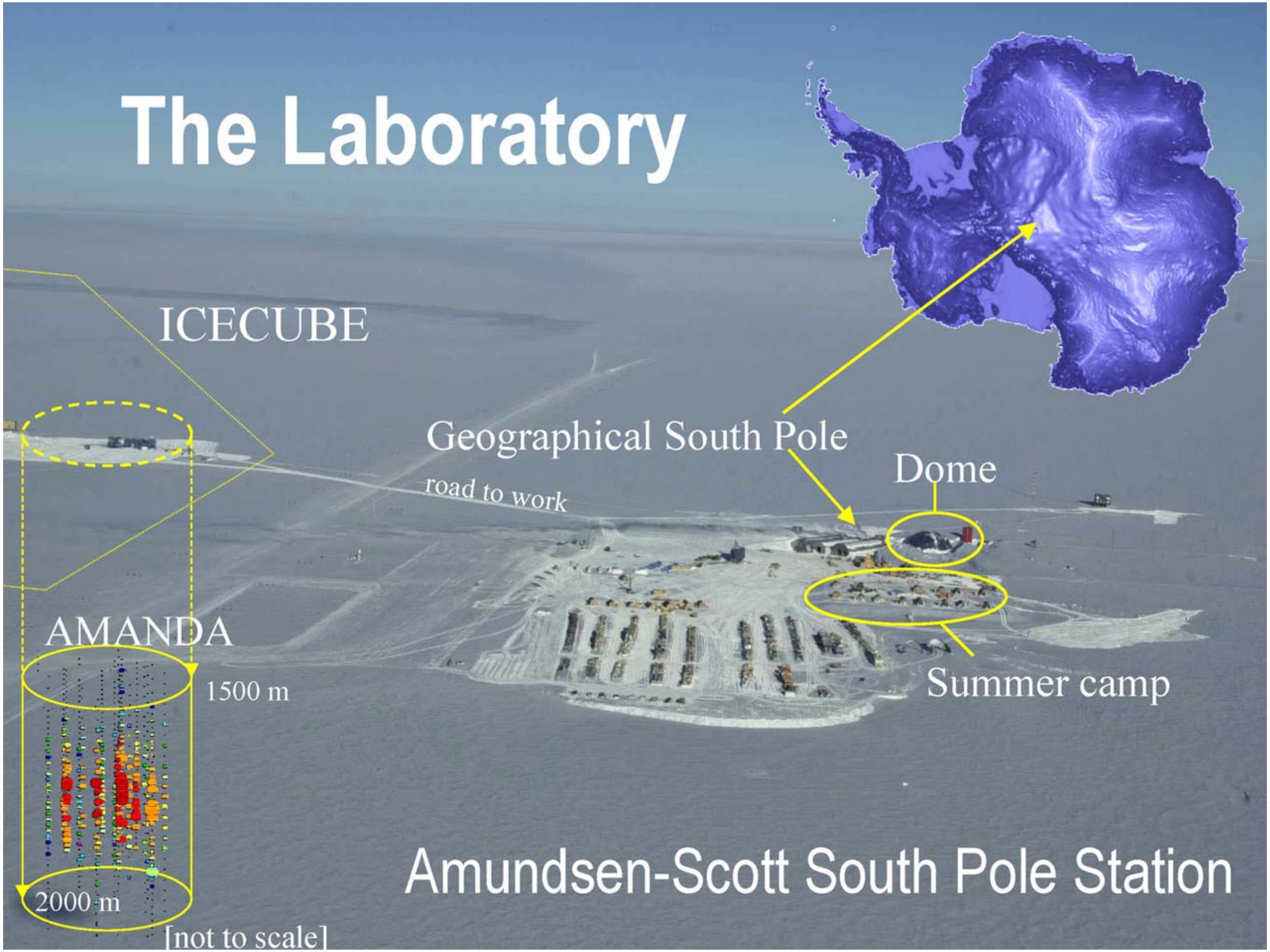
The Laboratory
ICECUBE
Geographical South Pole
Dome
road to work
AMANDA
1500 m
Summer camp
2000 m
[not to scale]
Amundsen-Scott South Pole Station

Ice optical properties

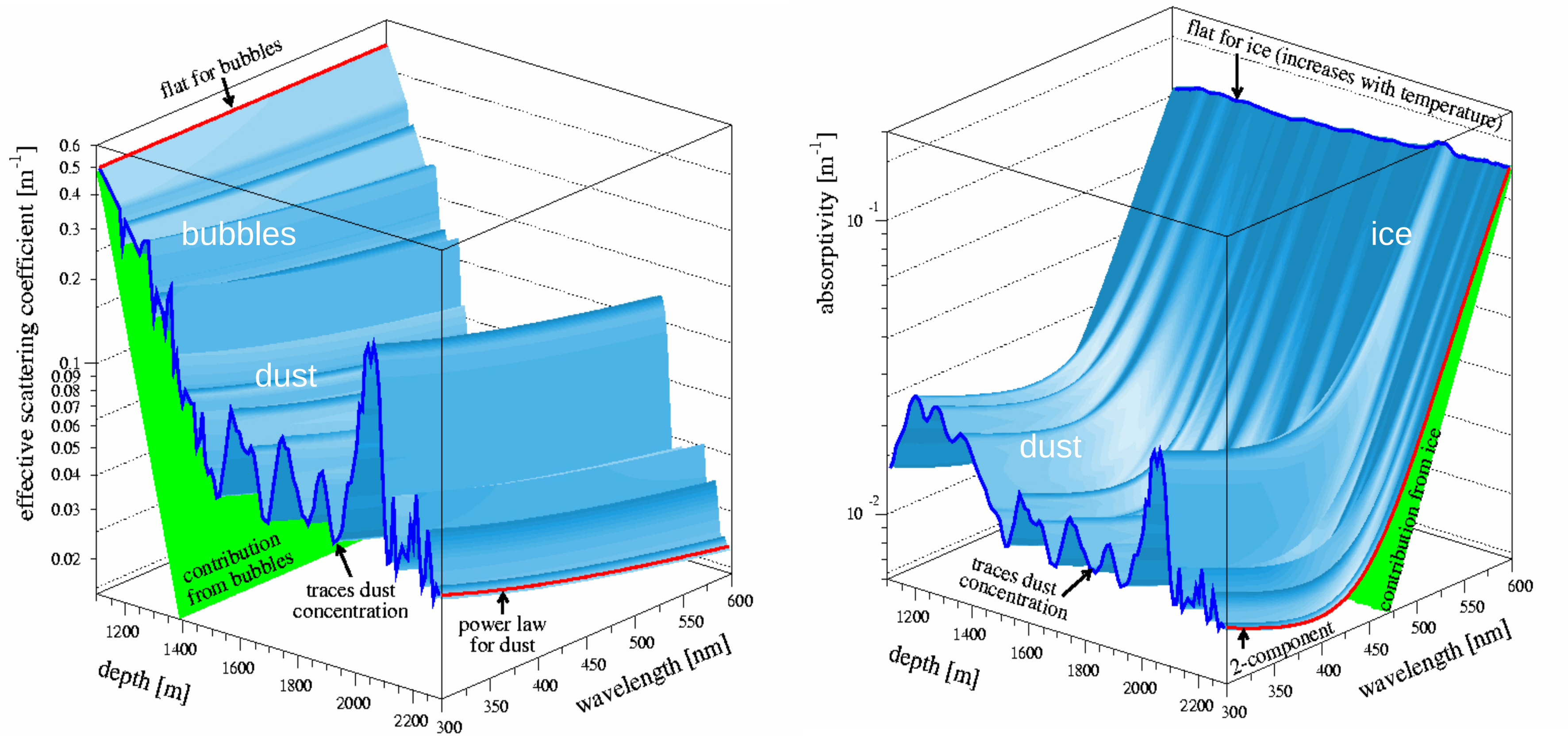

From in-situ light emitters	
	Length (m) @ λ= 400 nm
Effective scattering	20
Absorption	110

M. Ackermann, et al., “Optical properties of deep South Pole Ice”, sub. to J. of Geophys. Res.

Amanda

Atmospheric neutrino spectrum

… as a test beam for the AMANDA detector

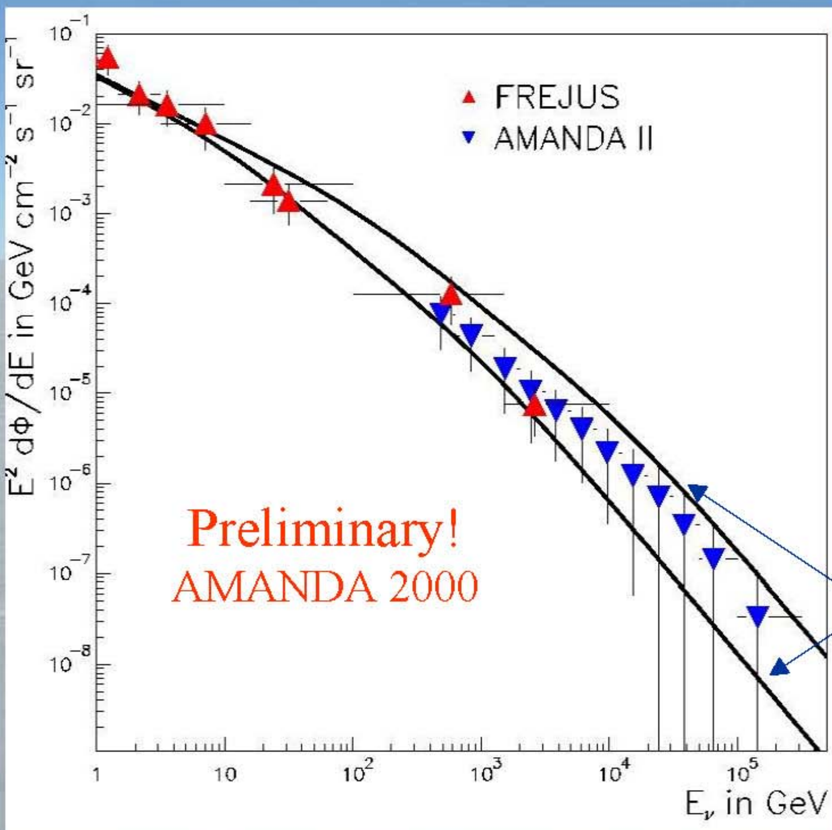

- Background of down-going atmospheric muons $10^6 \times$ more abundant
- Energy reconstruction based on neural network and regularized unfolding
- First energy spectrum > 1 TeV
- Matches lower-energy Frejus data
- Compatible with expectation of atmospheric neutrino flux

Spectrum is used to study excess due to cosmic neutrinos

Atmospheric neutrinos – the angular distribution

- Preliminary investigation with AMANDA (year 2002 data):
  - competitive with MACRO if uncertainties (syst. and stat.) are low:
    - < 30 % flux
    - < 5 % zenith shape
    - 4 years statistics (~ 4000 events)
- IceCube: 2 orders of magnitude improvement in sensitivity

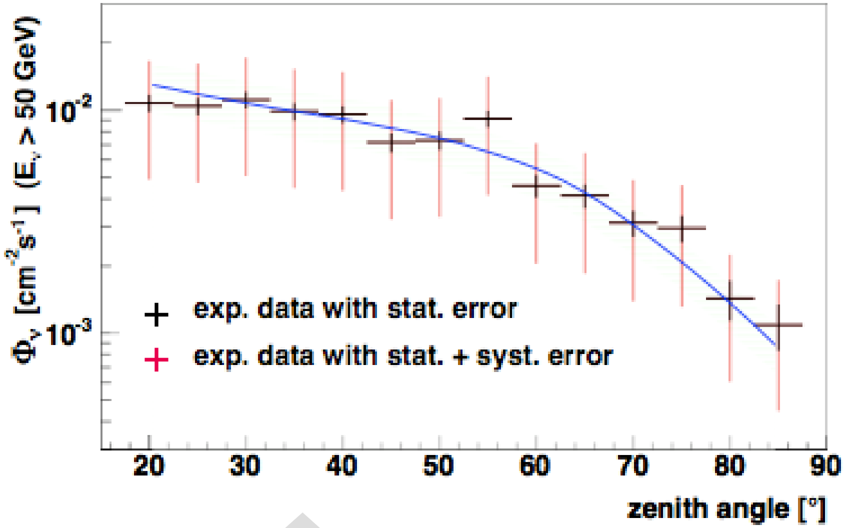

Atmospheric muon neutrino flux (E>50 GeV). Line: Monte Carlo prediction (incl. oscillations)

Atmospheric neutrinos – the spectrum

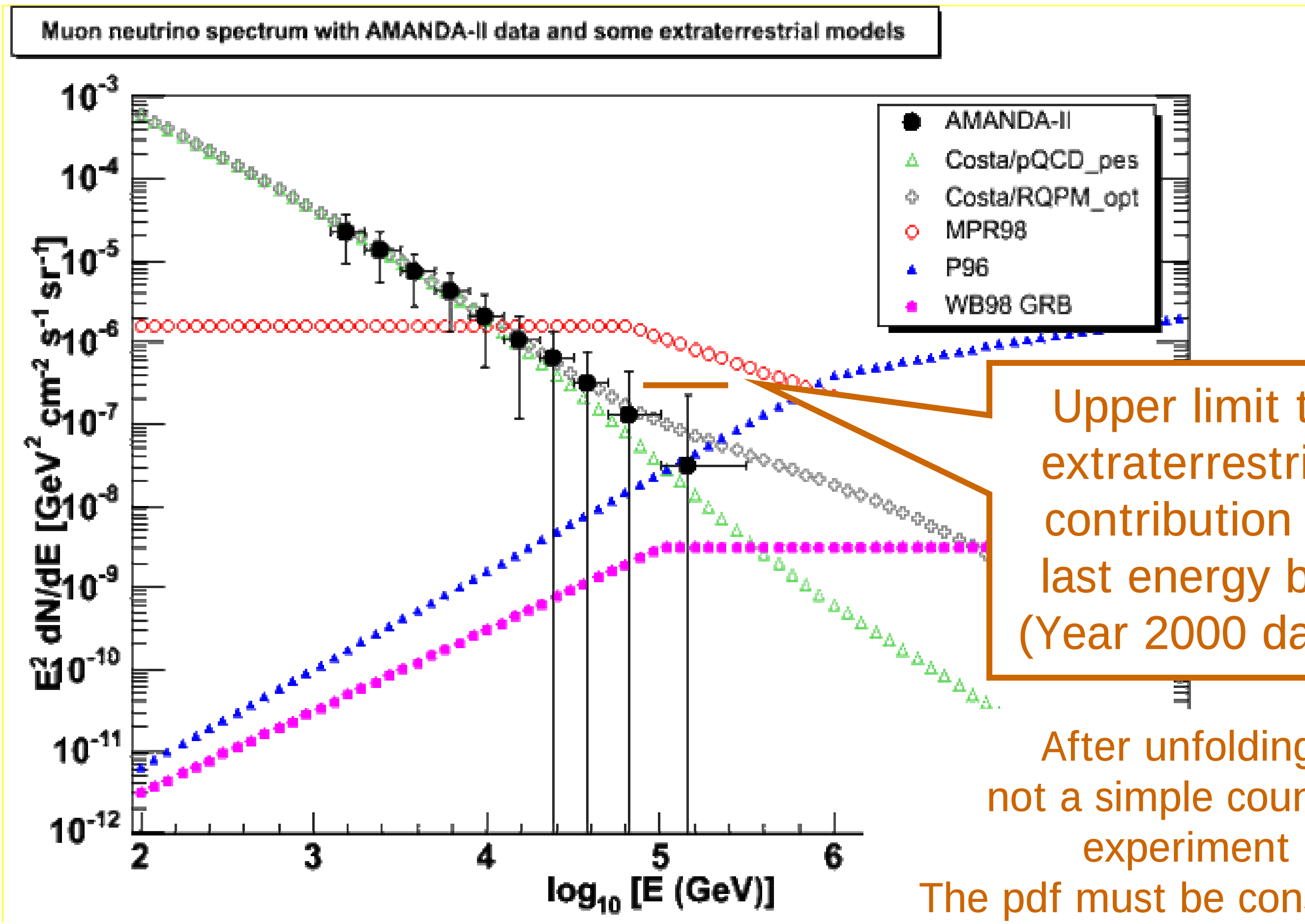

Upper limit to extraterrestrial contribution in last energy bin (Year 2000 data)

After unfolding: not a simple counting experiment
The pdf must be constructed from signal Monte Carlo simulations

H. Geenen *et. al,* 28th ICRC, Tsukuba (2003)
K. Muenich *et. al,* 29th ICRC, Pune (2005)

Amanda

Search for extraterrestrial point sources

→ Look for an excess of up-going muon tracks in particular directions in the sky (sky bins)

- Grid search: sky subdivided into 300 bins (~7°*7°)
- Optimization of cuts in each declination band

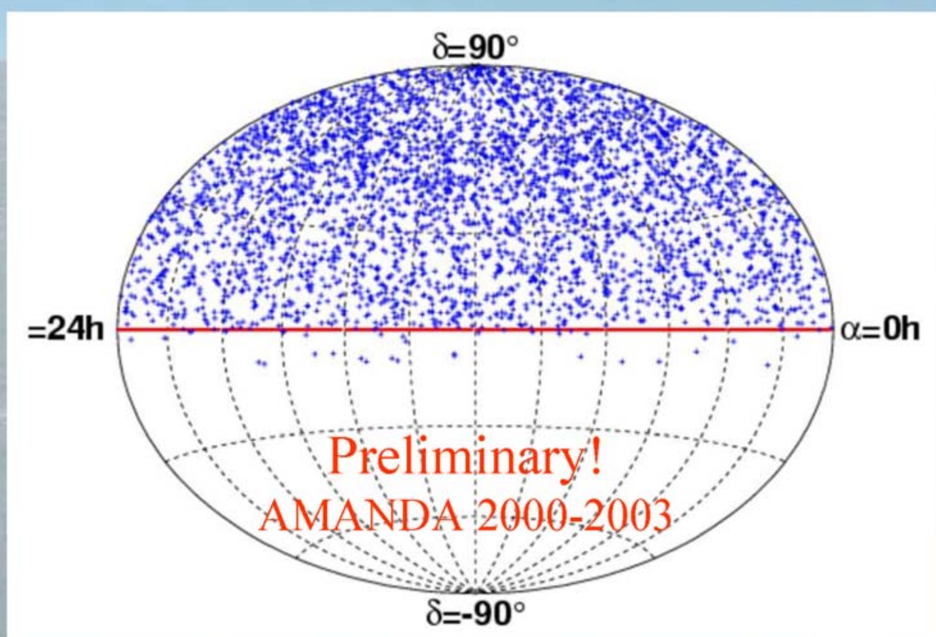

- 3369 neutrino events observed from below the horizon, while 3438 expected from atmospheric neutrino simulation

No clustering observed

⇓

No evidence for point sources

Search for extraterrestrial point sources

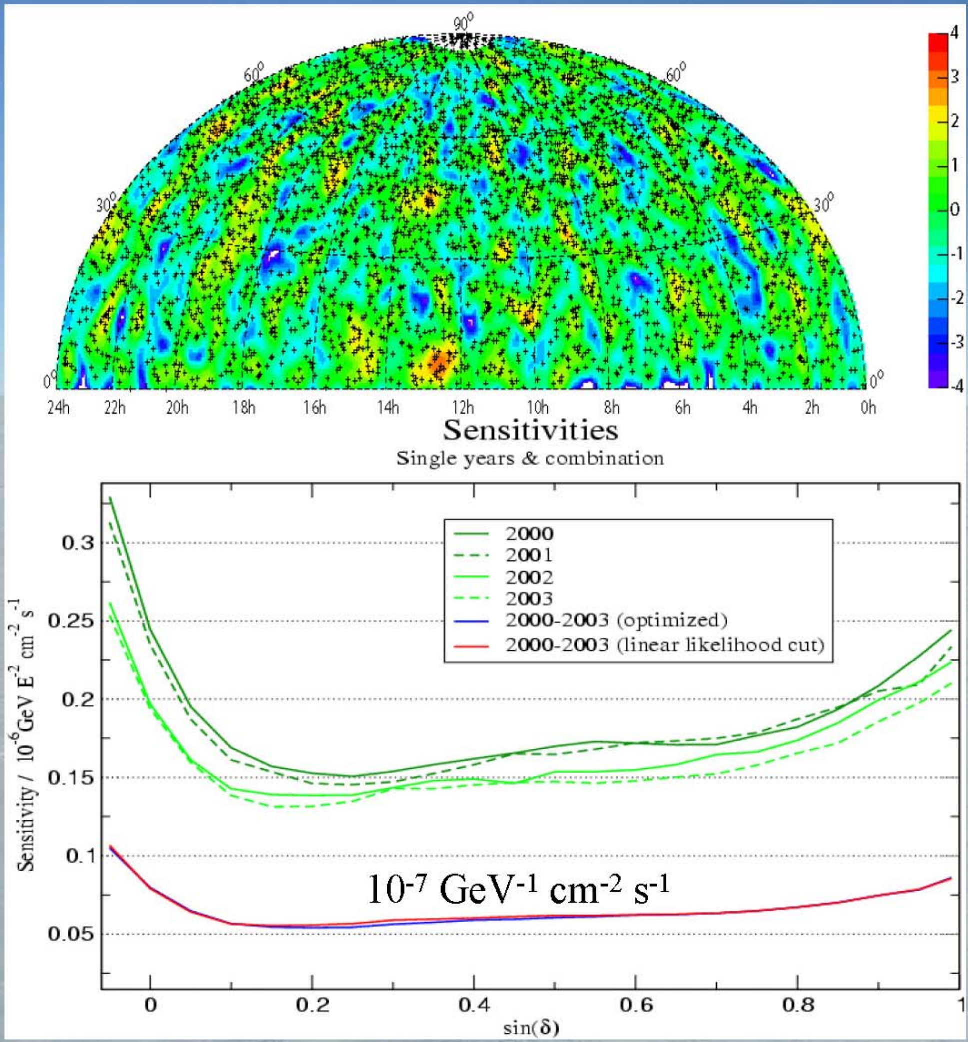

- Significance of local fluctuations compared to expectation of all being atmospheric neutrinos

➔ max 3.4 σ

⇒ compatible with bg fluctuation

- Improved sensitivity for full data set (2000-2003)
- 807 days of live time

published results

Data 1997 : Ap.J. 583, 1040 (2003)

Data 2000 : PRL 92, 071102 (2004)

Statistical test of 33 pre-selected objects

	Source	Nr. of ν events	Expected background	$\Phi_{90\%}(E_\nu>10\ \mathrm{GeV})$ $[10^{-8}\mathrm{cm}^{-2}\mathrm{s}^{-1}]$
TeV Blazars	**Markarian 421**	6	5.6	0.7
	Markarian 501	5	5.0	0.6
	1ES 1426+428	4	4.3	0.5
	1ES 2344+514	3	4.9	0.4
	1ES 1959+650	5	3.7	1.0
GeV Blazars	**QSO 0528+134**	4	5.0	0.4
	QSO 0235+164	6	5.0	0.7
	QSO 1611+343	5	5.2	0.6
	QSO 1633+382	4	5.6	0.4
	QSO 0219+428	4	4.3	0.5
	QSO 0954+556	2	5.2	0.2
	QSO 0716+714	1	3.3	0.3
MicroQuasars	**SS433**	2	4.5	0.2
	GRS 1915+105	6	4.8	0.7
	GRO J0422+32	5	5.1	0.6
	Cygnus X-1	4	5.2	0.4
	Cygnus X-3	6	5.0	0.8
	XTE J1118+480	2	5.4	0.2
	CI Cam	5	5.1	0.7
	LSI +61 303	3	3.7	0.6
SNRs	**SGR 1900+14**	3	4.3	0.4
	Crab Nebula	**10**	**5.4**	1.3
	Cassiopeia A	4	4.6	0.6
	Geminga	3	5.2	0.3


= 2.25°-3.75°

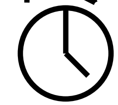
= 807 days

The statistical significance is evaluated with MC experiments on events with randomized right ascension

The chance probability of such an excess (or higher) in any of the 33 objects is **64%**

Search for time variable signals - ν flares

Search for ν flares using time-sliding windows:

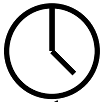
= 40/20 days for Extragalactic/Galactic Objects

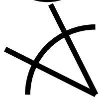
= 2.25°-3.75°

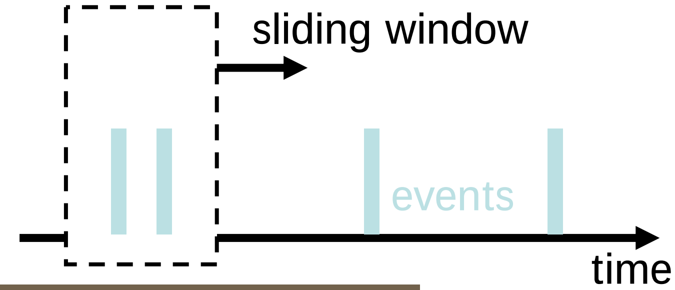

Source	Period duration	Nr. of doublets	Probability for highest multiplicity
Markarian 421	40 days	0	Close to 1
1ES1959+650	40 days	1	0.34
3EG J1227+4302	40 days	1	0.43
3EG J0450+1105	40 days	1	0.47
QSO 0235+164	40 days	1	0.52
QSO 0528+134	40 days	0	Close to 1
Cygnus X-3	20 days	0	Close to 1
Cygnus X-1	20 days	0	Close to 1
GRS 1915+105	20 days	1	0.32
GRO J0422+32	20 days	0	Close to 1
3EG J1828+1928	20 days	0	Close to 1
3EG J1928+1733	20 days	1	0.35

Observations from the direction of 1ES 1959+650

An interesting coincidence with a gamma-ray flare:

5 events observed compared to **3.7 background** expected from atmospheric neutrinos, between 2000 and 2003.

3 events are within 66 days in 2002, partly overlapping a period of major activity of the source

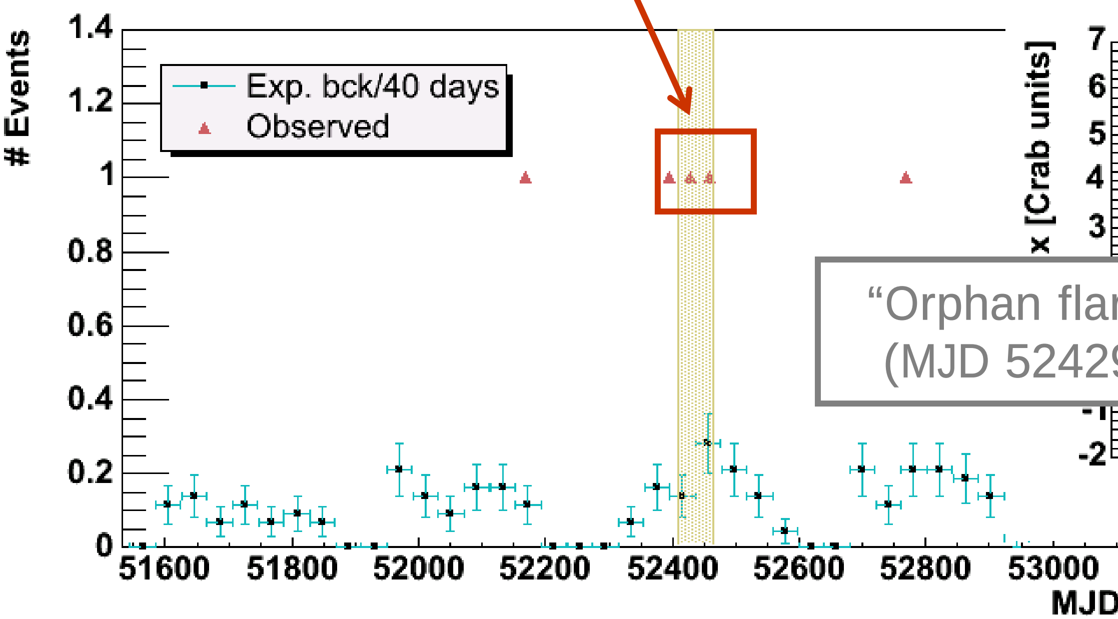

AMANDA events within 2.25º from the direction of 1ES 1959+650

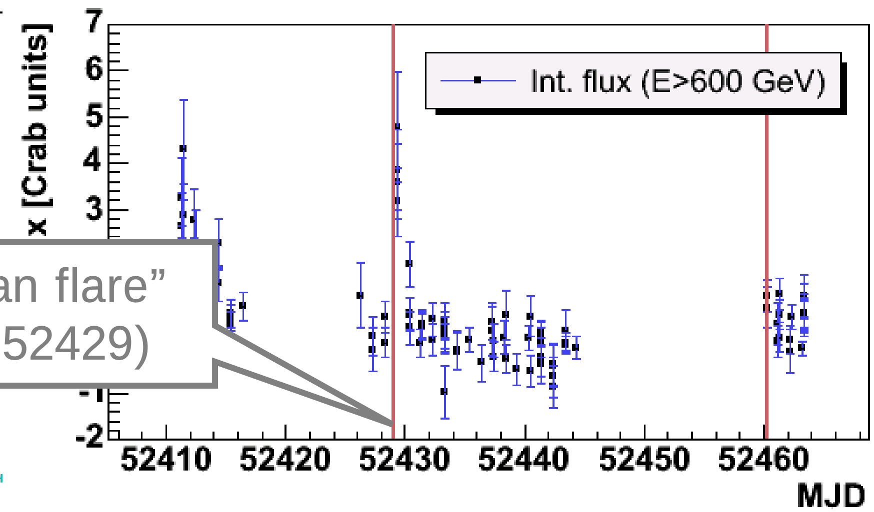

Whipple light curve [Holder et al 2003]

Amanda

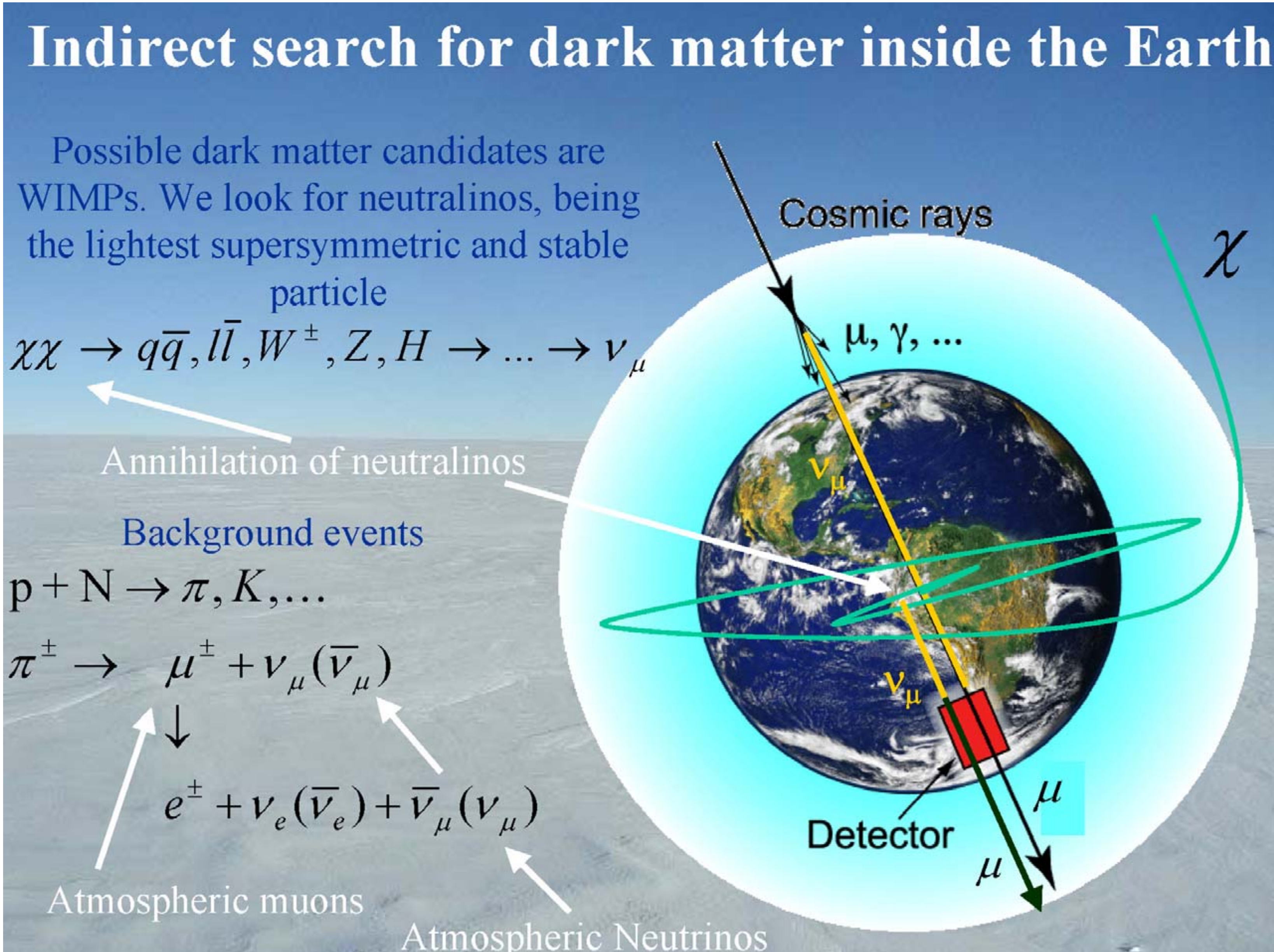
Indirect search for dark matter inside the Earth
Possible dark matter candidates are WIMPs. We look for neutralinos, being the lightest supersymmetric and stable particle
$\chi\chi \rightarrow q\bar{q}, l\bar{l}, W^{\pm}, Z, H \rightarrow \ldots \rightarrow \nu_{\mu}$
Annihilation of neutralinos
Background events
$\mathrm{p} + \mathrm{N} \rightarrow \pi, K, \ldots$
$\pi^{\pm} \rightarrow \mu^{\pm} + \nu_{\mu}(\bar{\nu}_{\mu})$
$\downarrow$
$e^{\pm} + \nu_e(\bar{\nu}_e) + \bar{\nu}_{\mu}(\nu_{\mu})$
Atmospheric muons
Atmospheric Neutrinos
Cosmic rays
$\mu, \gamma, \ldots$
χ
ν_{μ}
ν_{μ}
Detector
μ
μ

Sky observable by Neutrino Telescopes

AMANDA (South Pole)

ANTARES (43° North)

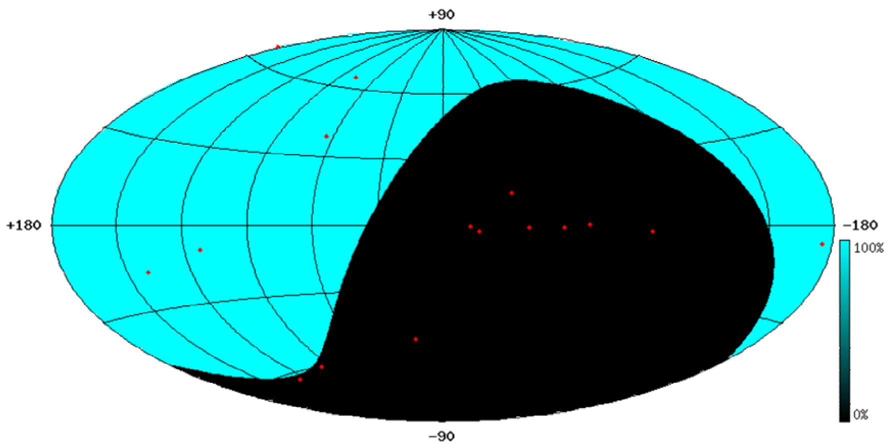

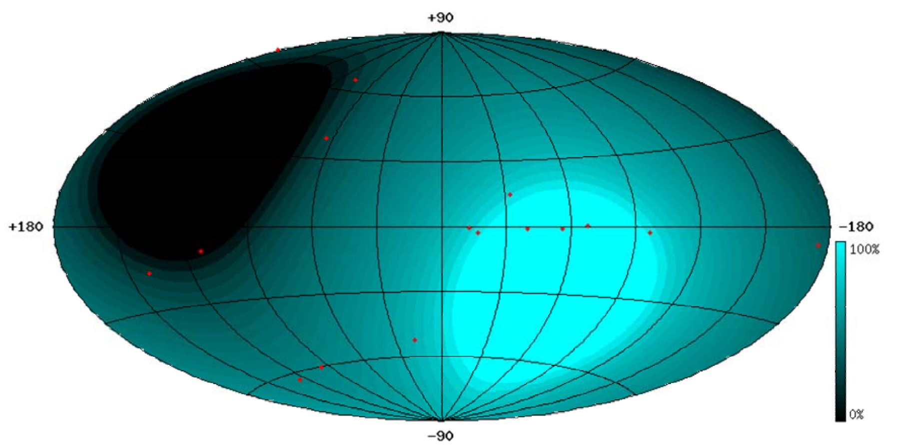

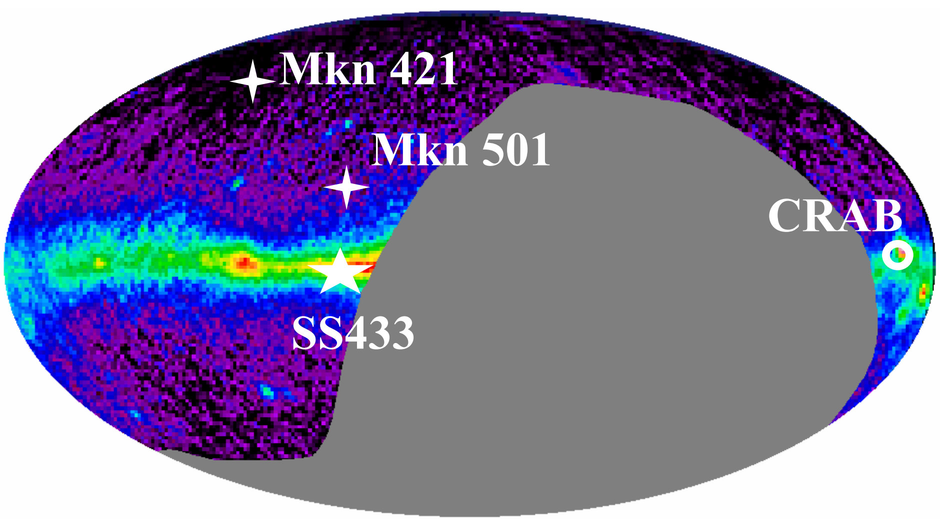

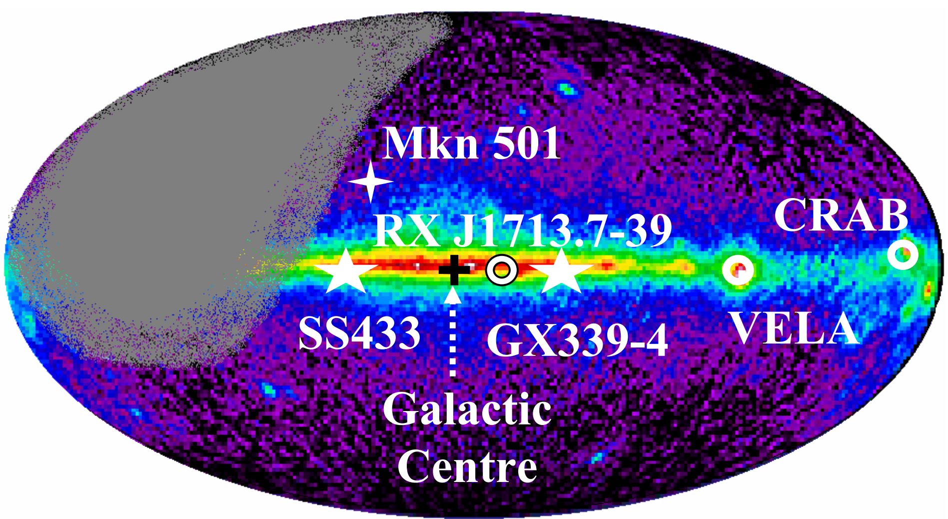

ANTARES Collaboration
150 Scientists and Engineers

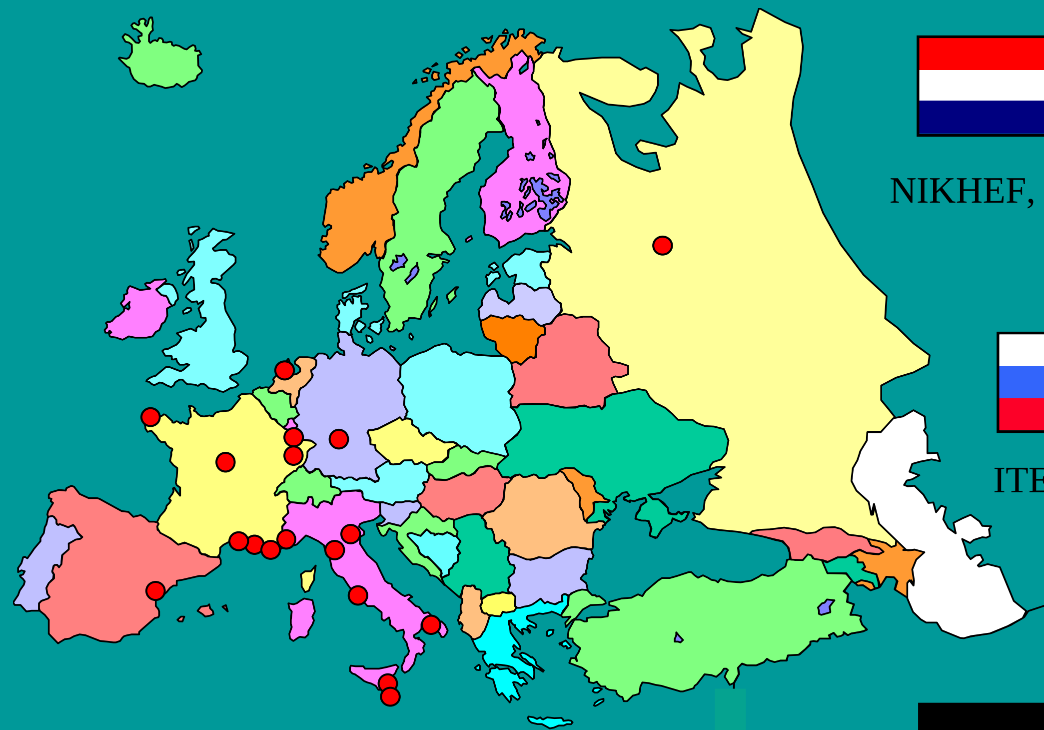

CPPM, Marseille
DSM/DAPNIA/CEA, Saclay
C.O.M. Marseille
IFREMER, Toulon/Brest
LAM, Marseille
IReS, Strasbourg
Univ. de H.-A., Mulhouse
ISITV, Toulon
LOV Villefranche

NIKHEF, Amsterdam

ITEP, Moscow

IFIC, Valencia

University Bari
University Bologna
University/LNS Catania
University Pisa
University Rome
University Genova

University Erlangen

Site location

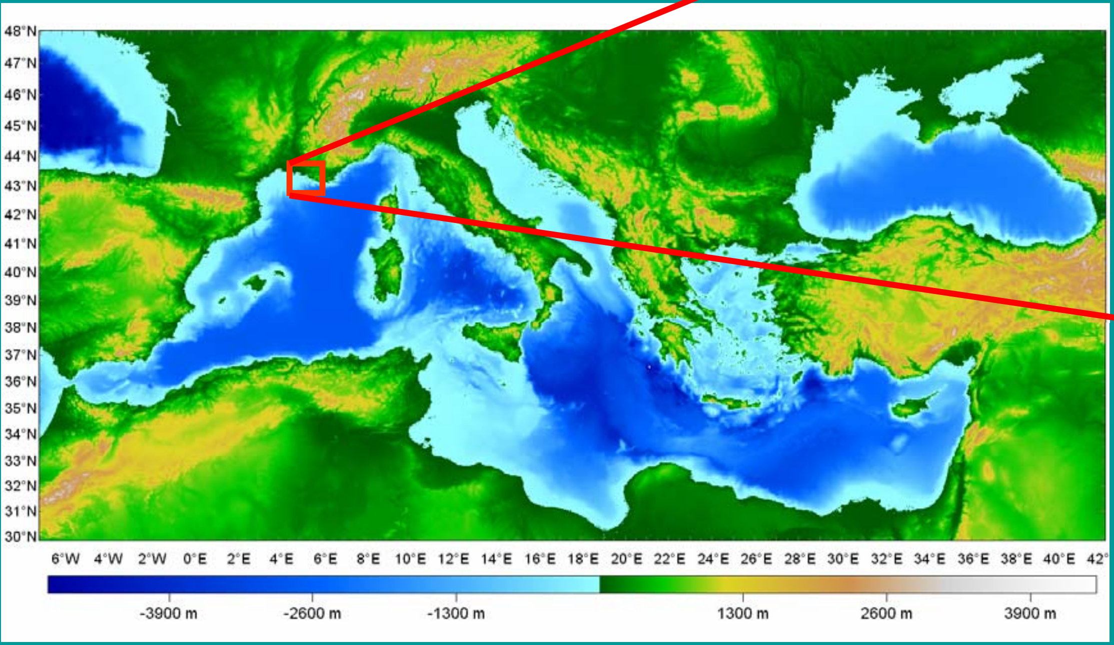

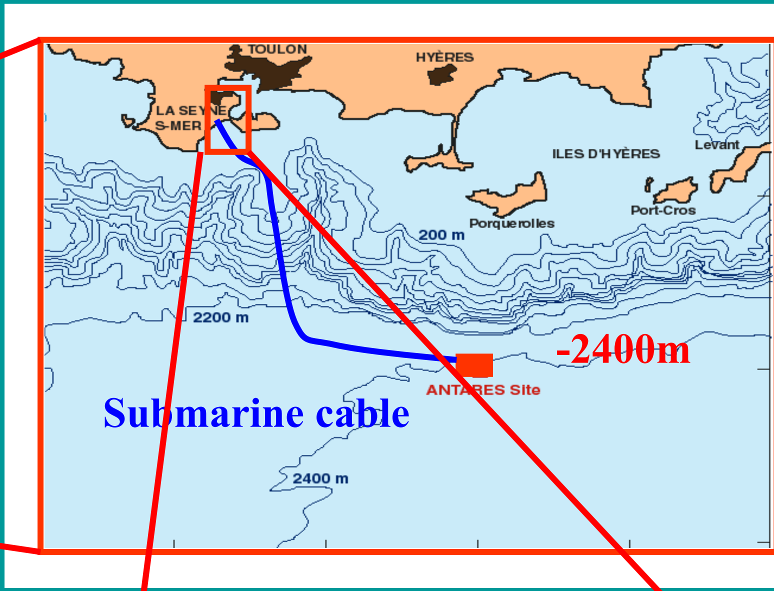

Shore Station

ANTARES test sites

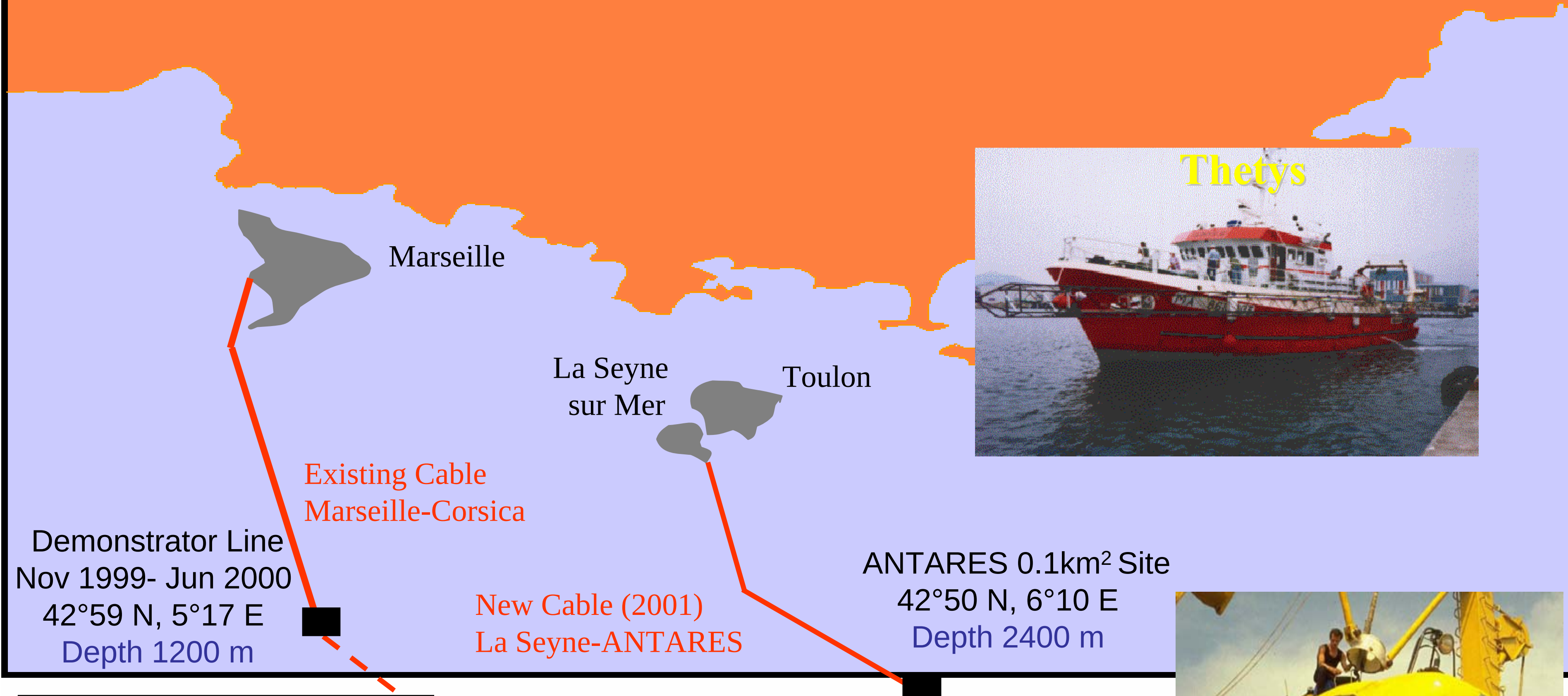

~ 40 deployments and recoveries of test lines for site exploration.

Biofouling

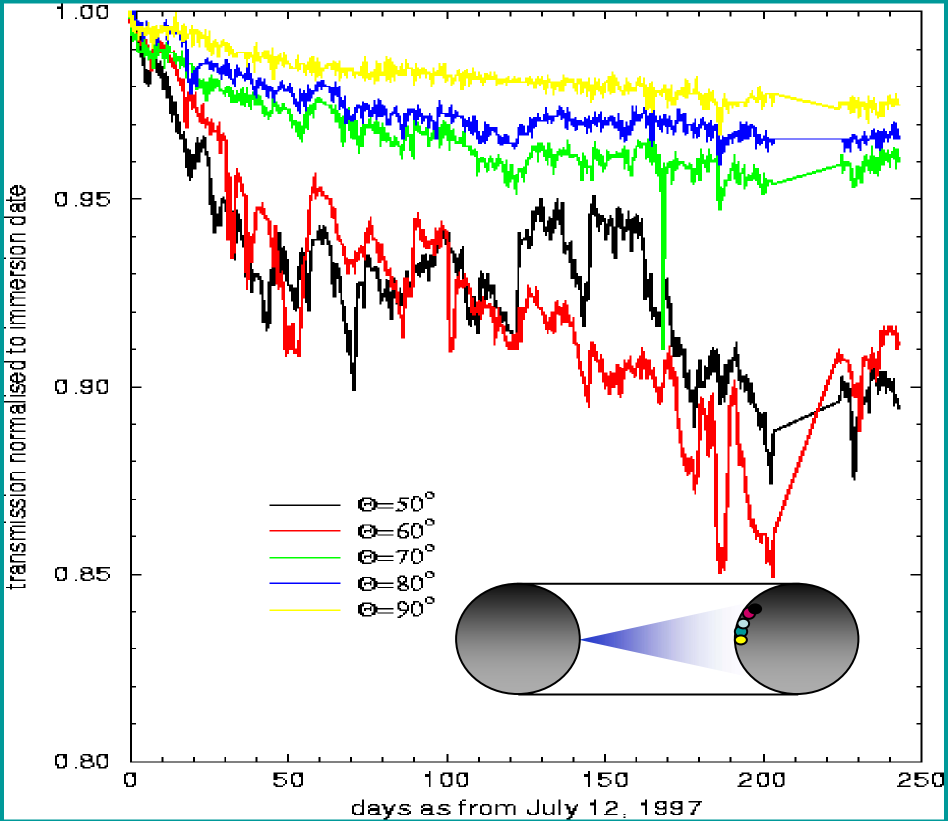

For θ > 90º transmission loss <1.5% in 1 yr (and saturates)

Optical Backgrounds

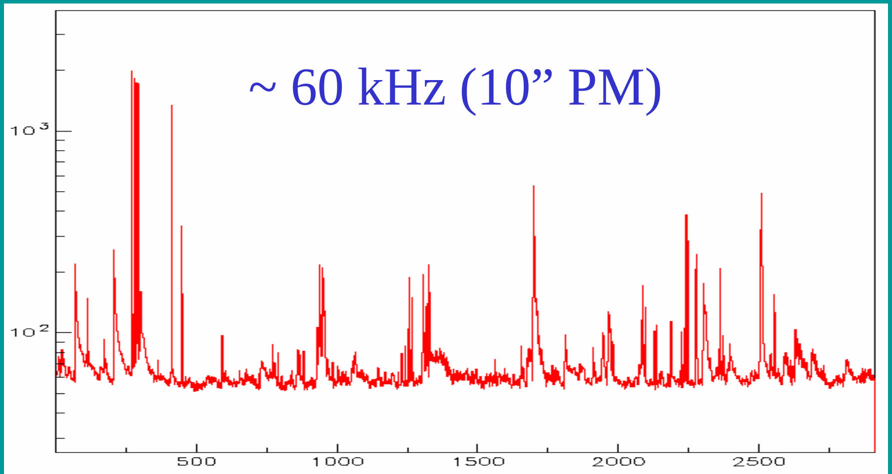

Short bursts (bioluminescence) over a continuous background (^{40}K).

~5% of time a PMT is unusable

Bioluminescent bacteria

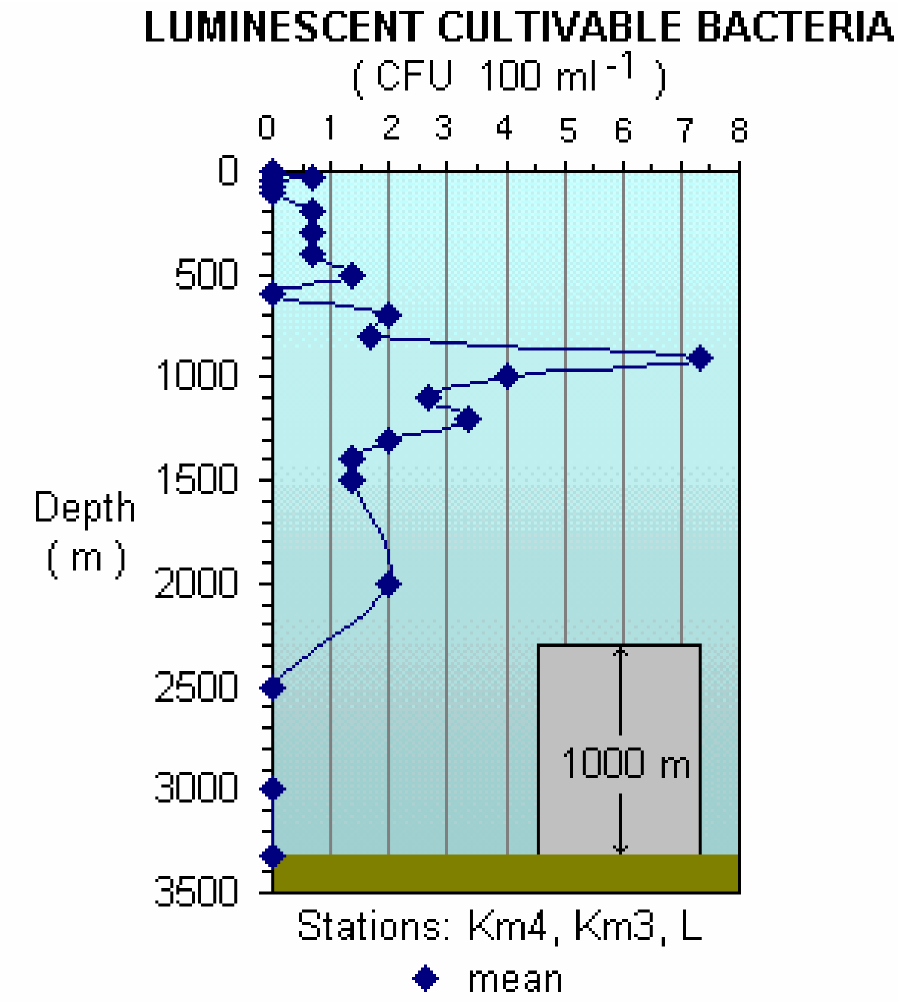

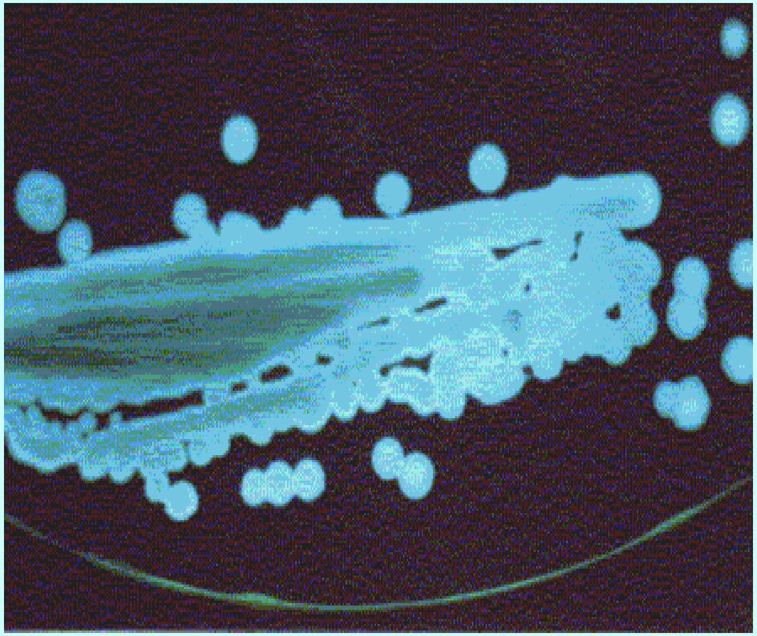

Bioluminescent bacteria on SWC

ANTARES Detector

12 strings
75 10” PM’s per string (PM’s at 45^0 wrt sea-bed)
Arranged in groups of 5 triplets (storeys) per section
5 sections/string

Storeys are 14.5 m apart. Interconnected by electro-optical cables providing: power, control signals, data transmission
Local Control Modules (LCM) connected to String Control Module (SCM) (Bottom of string)
SCM connected to Junction Box
JB connected to submarine cable

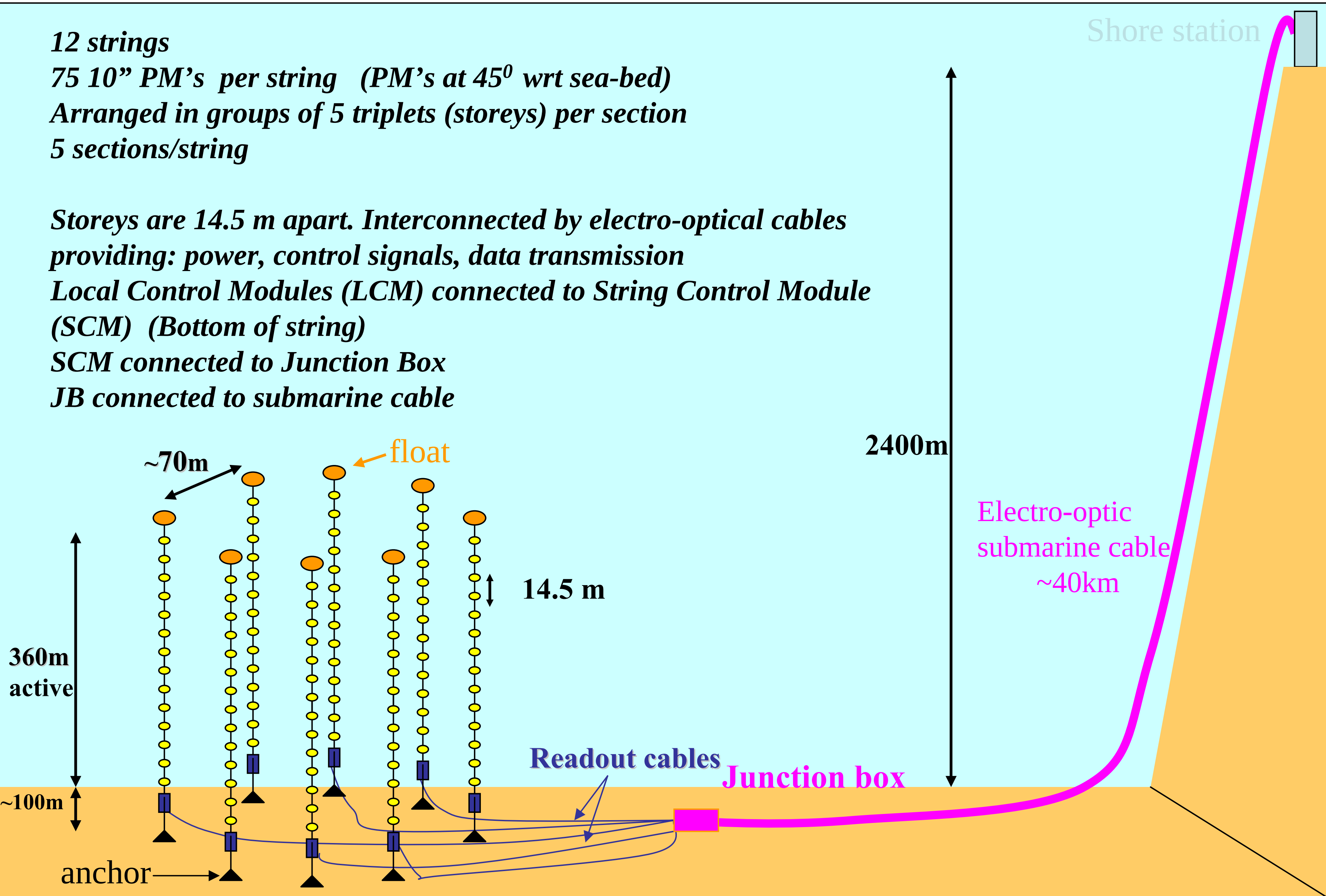

Detector layout

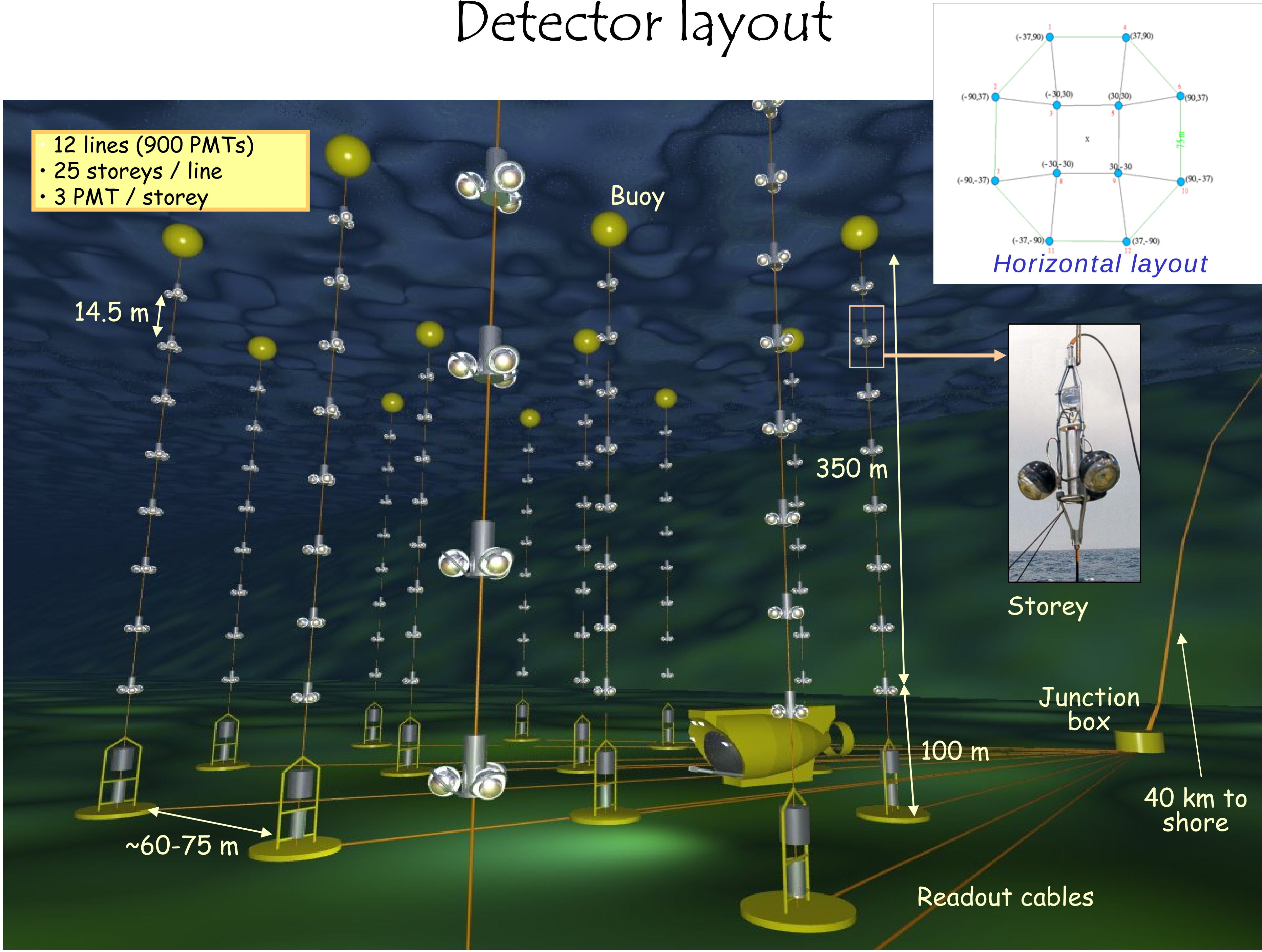

Detector design

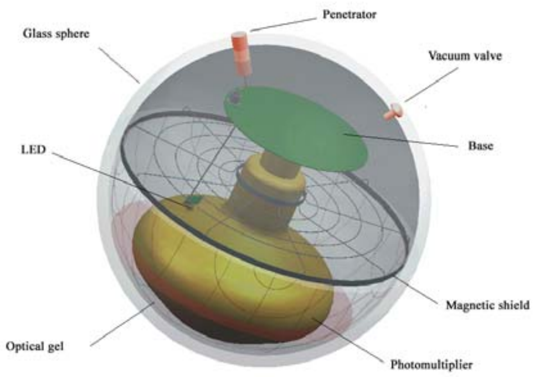

The Optical Module contains a 10’’ PMT and the associated electronics.
An internal LED will monitor the transit time of the PMT.

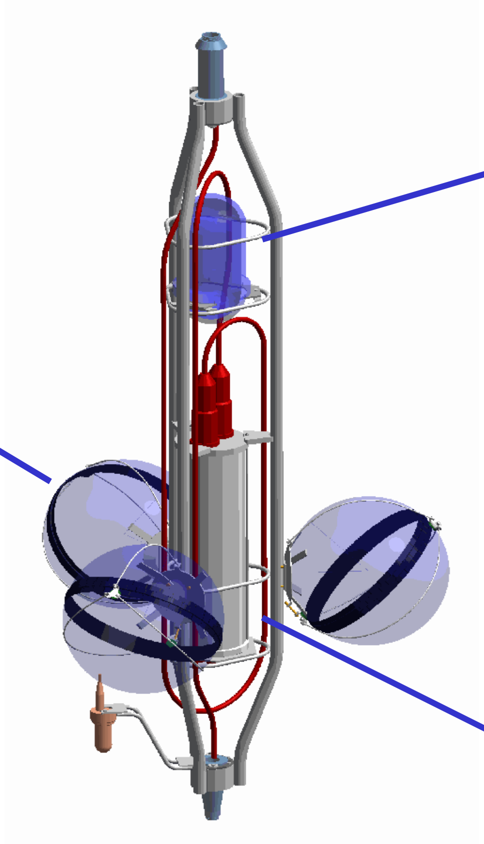

The storey

The Optical Beacons will allow the timing calibration of the detector with external sources (blue LEDs)

The Local Control Module processes PMT signals. The electronics is housed in a Ti cylinder.

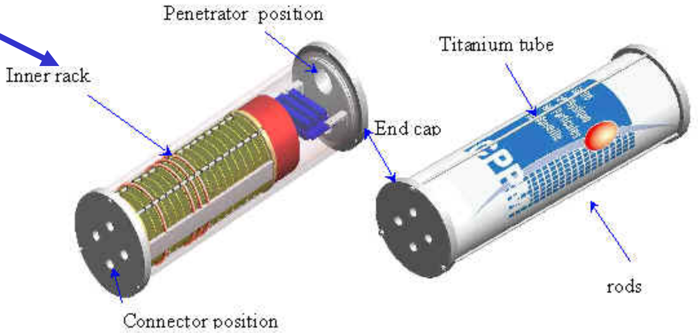

Prototype Line ready: Nov 2002

Line Deployment 0.1km^2 Detector

Storeys deployed two by two

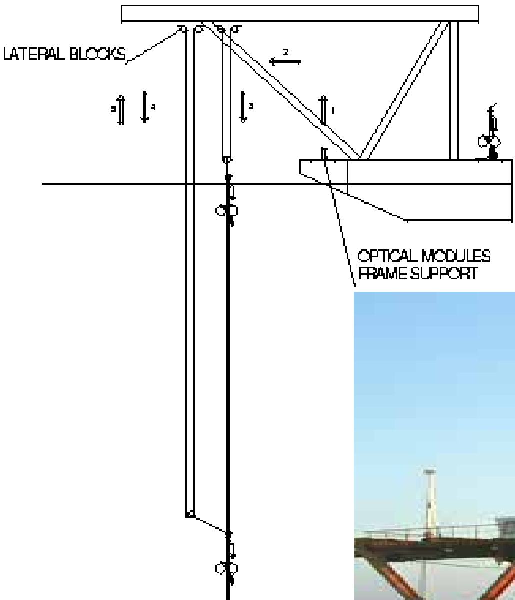

Storeys stored on deck of Castor

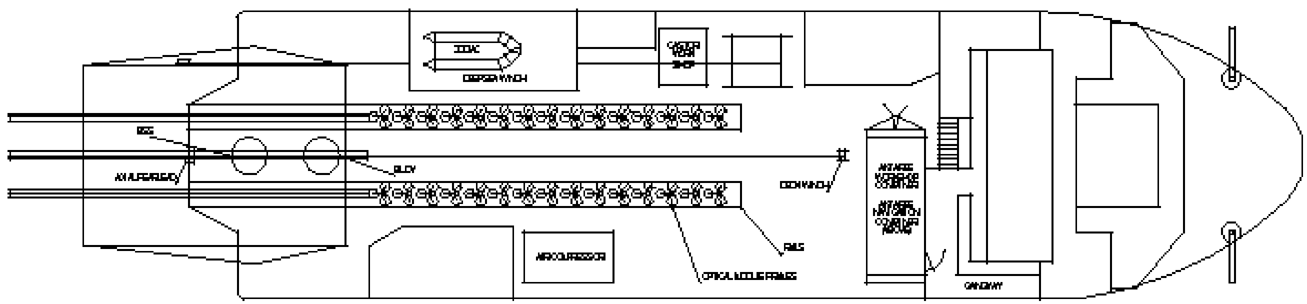

Nautile

Submarine cable connection

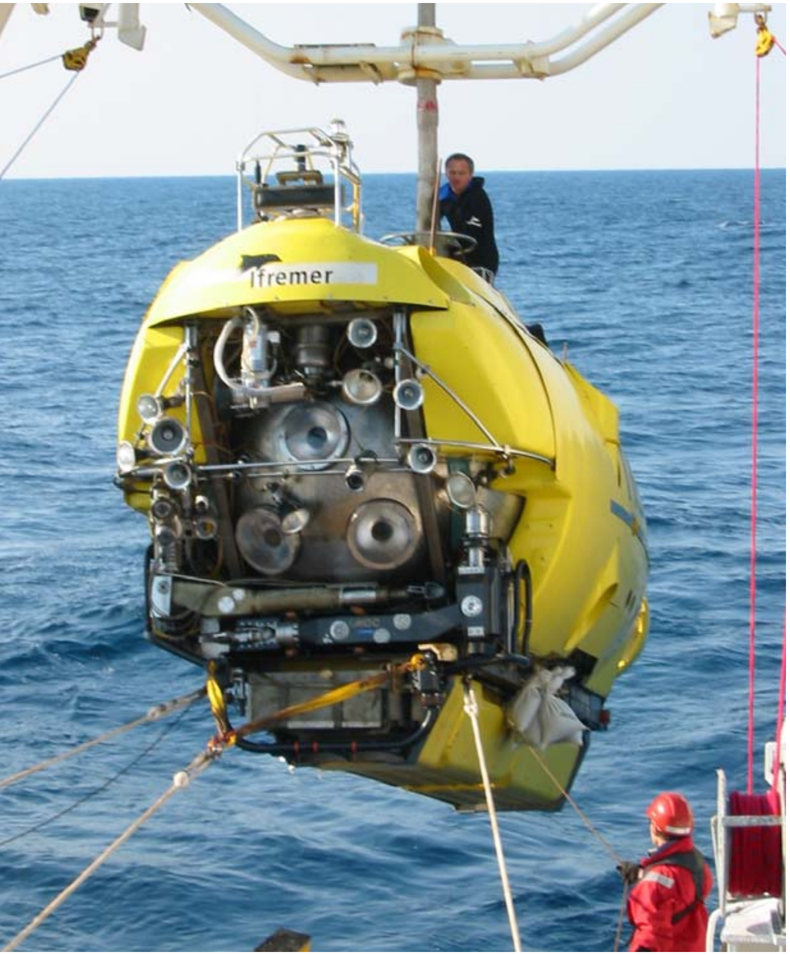

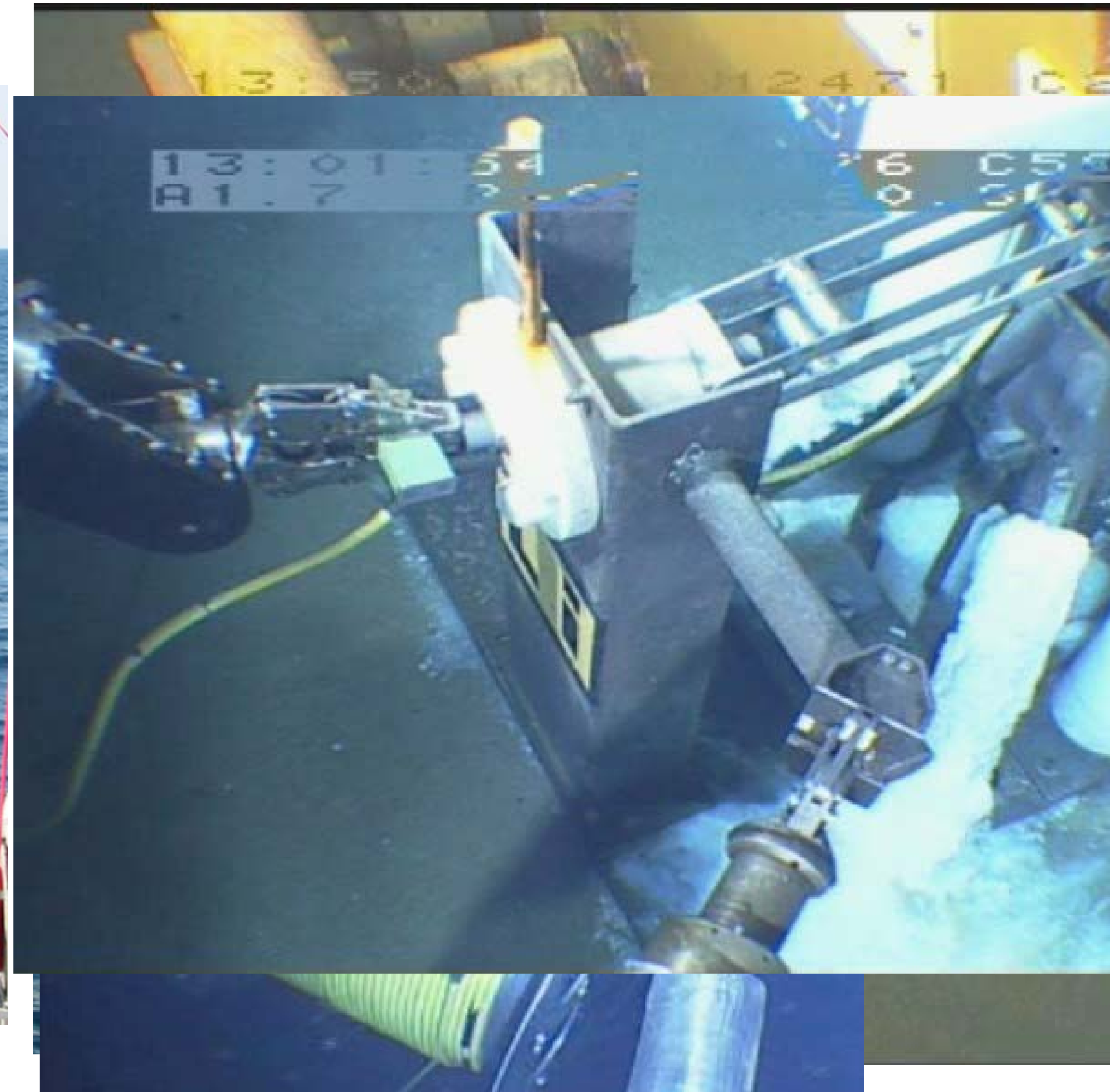

Current layout

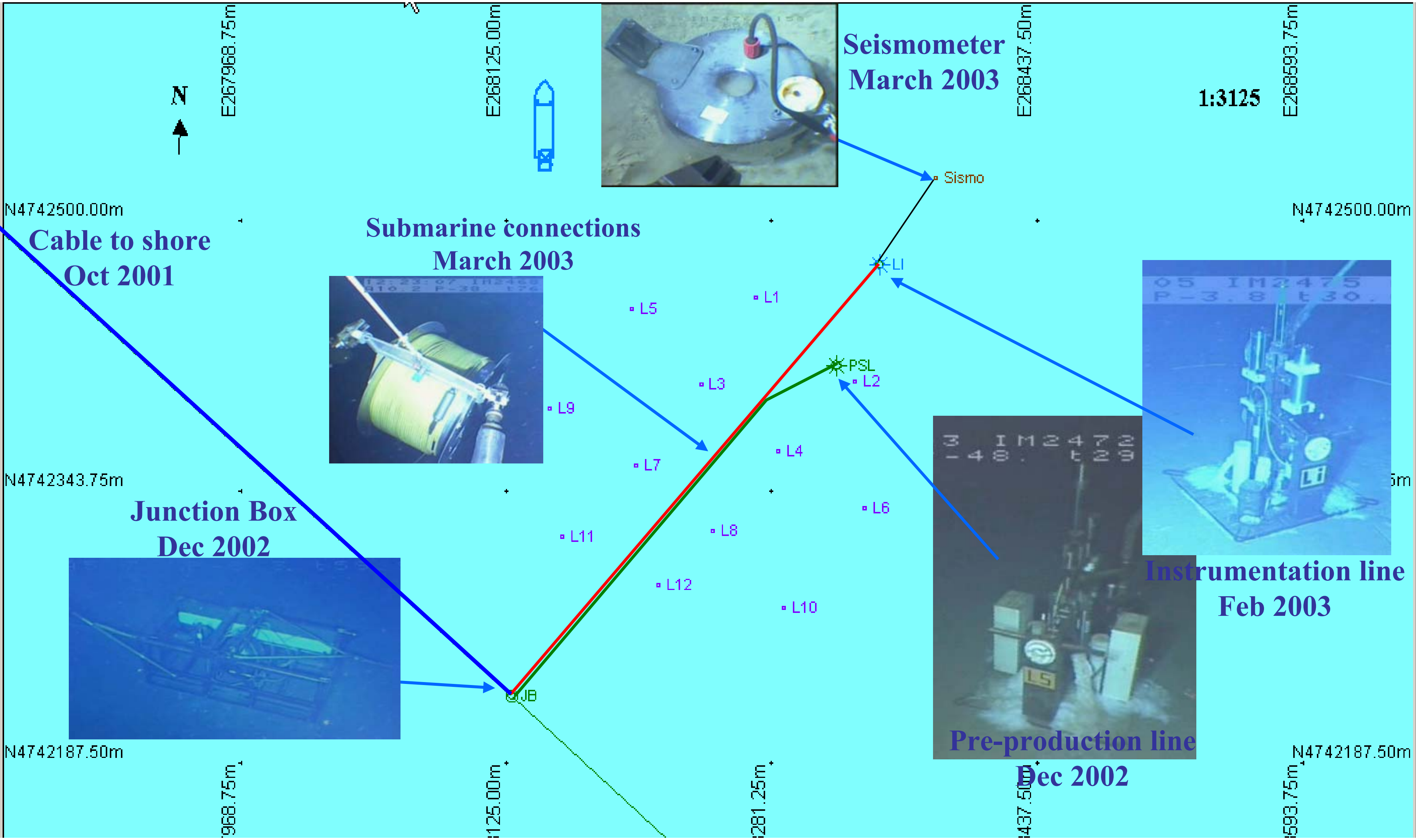

Inertial water motion

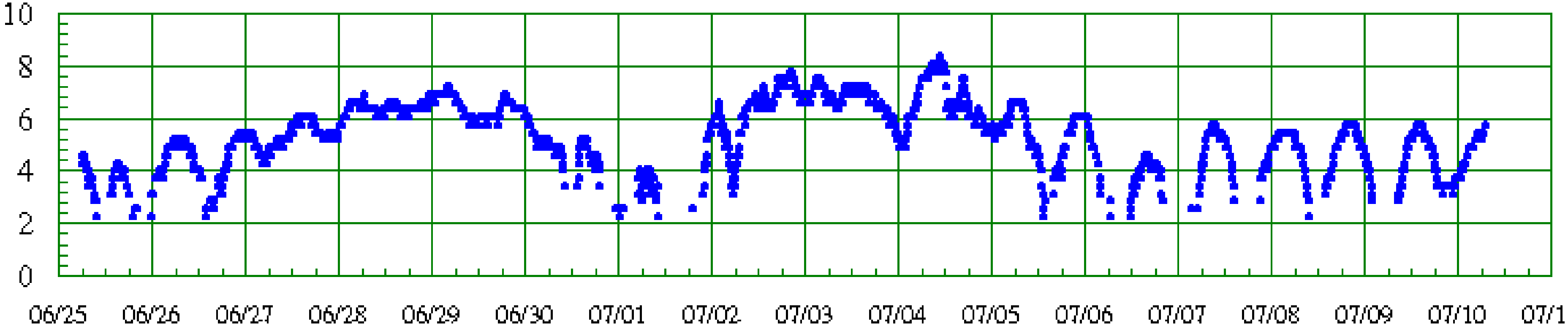

Coriolis effect

ν=2 ω sin ϕ with ϕ=42^{o} → **T=18 hr**

where ω is 2π/24 hr

Correlation with current speed

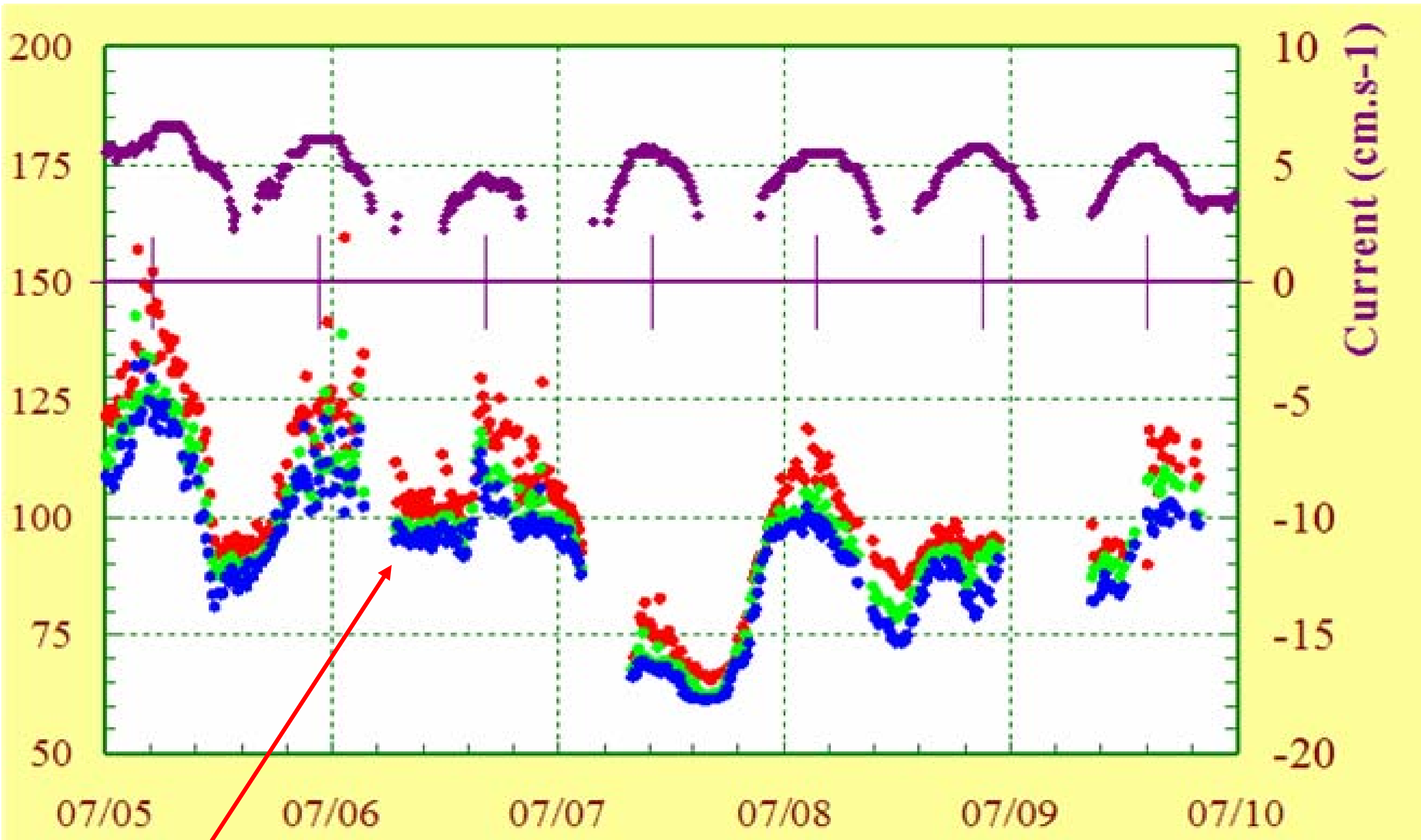

Attvita' ottica dovuta a bioluminescenza

Correlation plot

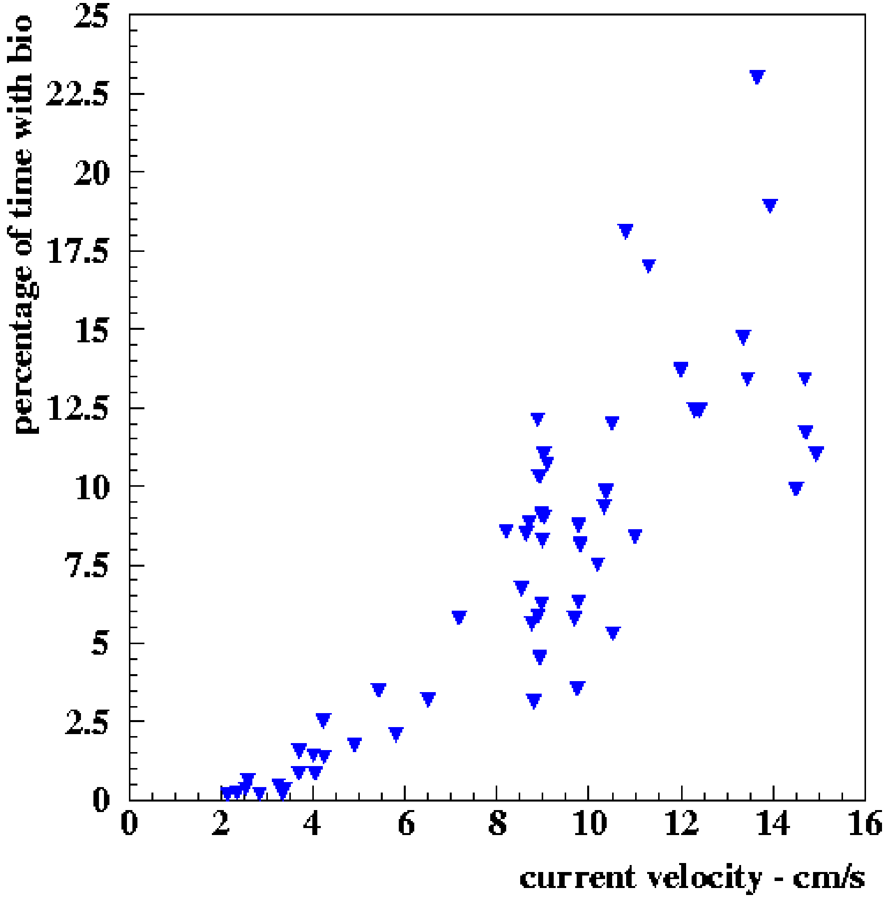

Expected performance

Angular resolution

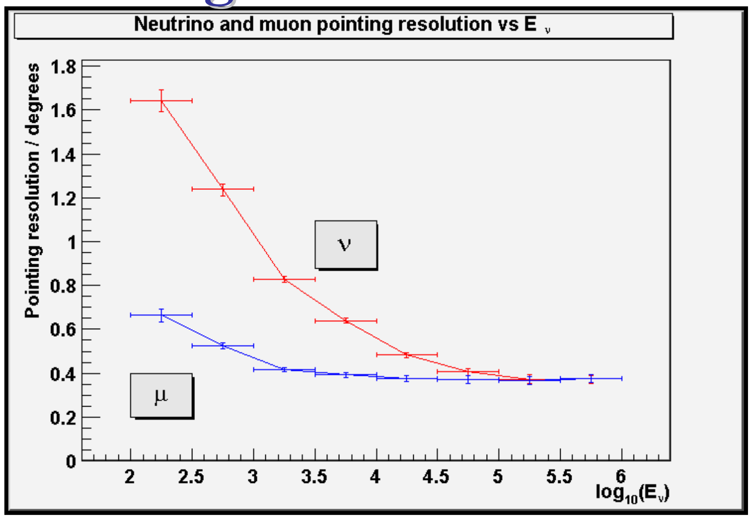

❖ Including effects of reconstruction and selection, PMT TTS, positioning, timing calibration accuracy and scattering.

❖ Below ~10 TeV angular error is dominated by ν-μ physical angle.

❖ Above ~10 TeV angular accuracy is better than 0.4° (reconstruction error).

Energy resolution

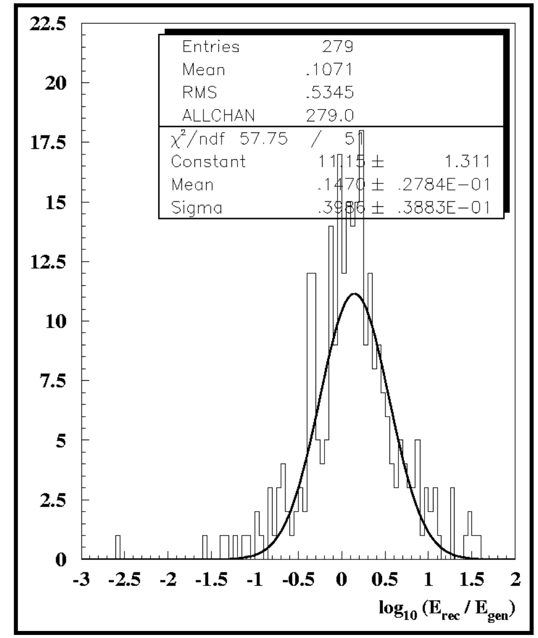

❖ $\sigma_E/E \approx 3$ (1 TeV≤ E ≤10 TeV)

❖ $\sigma_E/E \approx 2$ (E >10 TeV)

❖ Below E ~ 100 GeV energy estimation via muon range measurement.

Background

Two kinds of physical background:

- **Muons produced by cosmic rays in the atmosphere (detector deep in the sea and selection of up-going events).**
- **Atmospheric neutrinos (cut in energy and angle for point sources).**

$$p \to \pi^+(+K^+ \ldots) \to \mu^+ + \nu_\mu$$

$$\to e^+ + \overline{\nu}_\mu + \nu_e$$

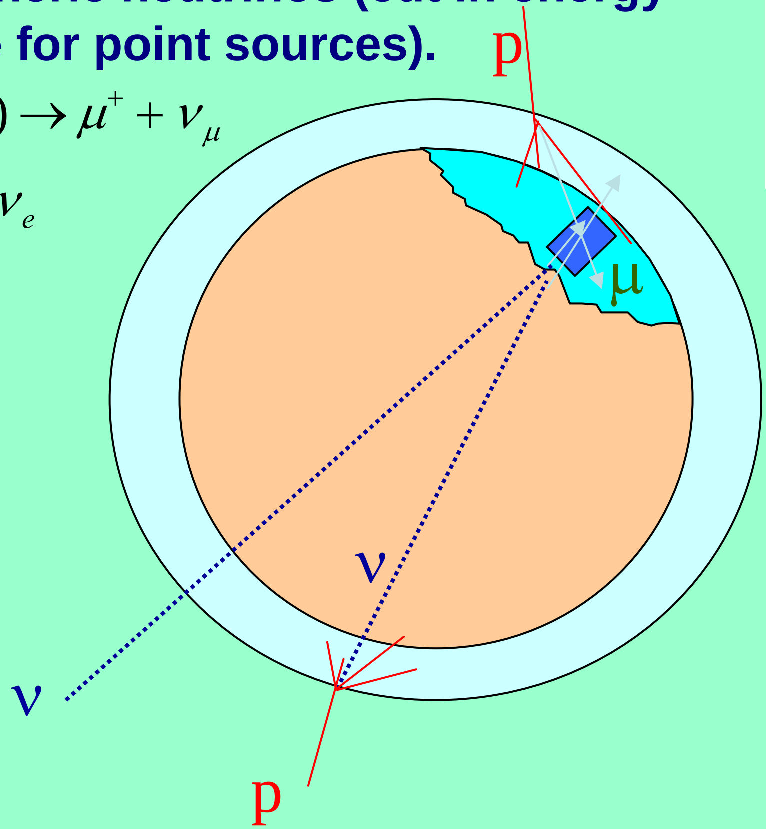

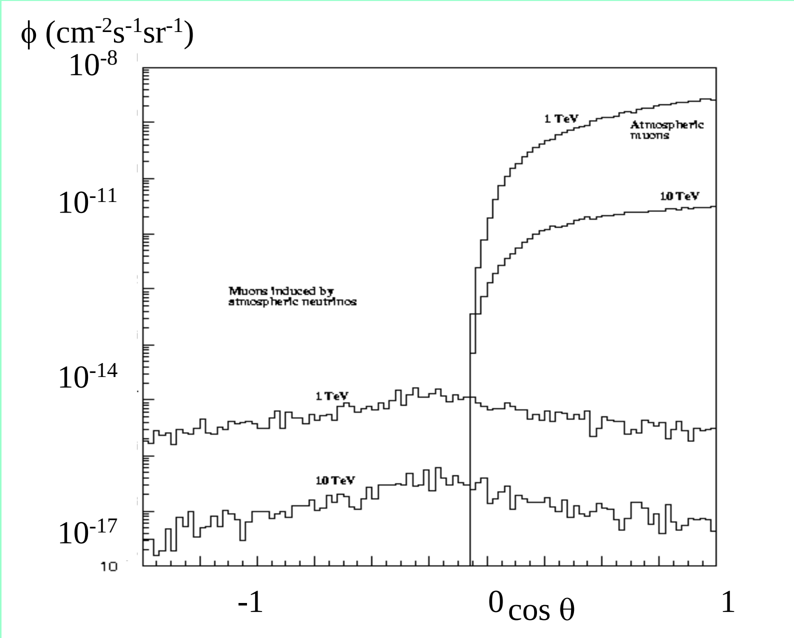

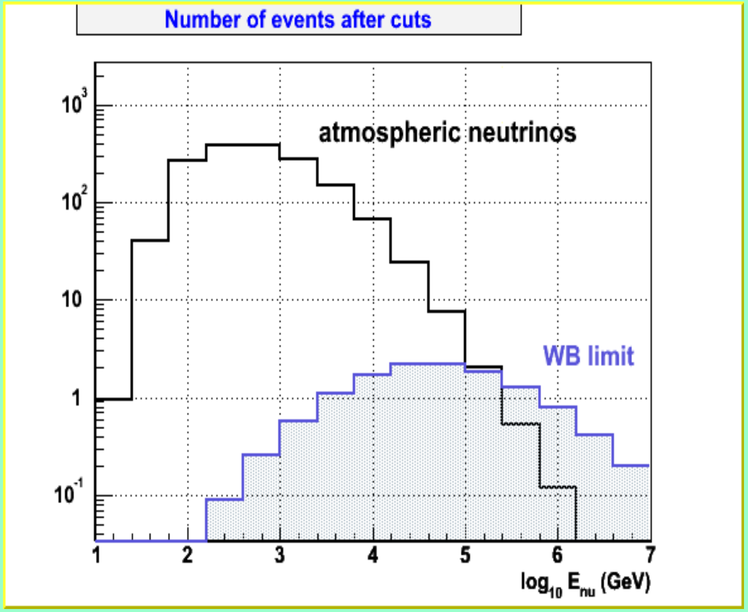

Muons seen by MACRO

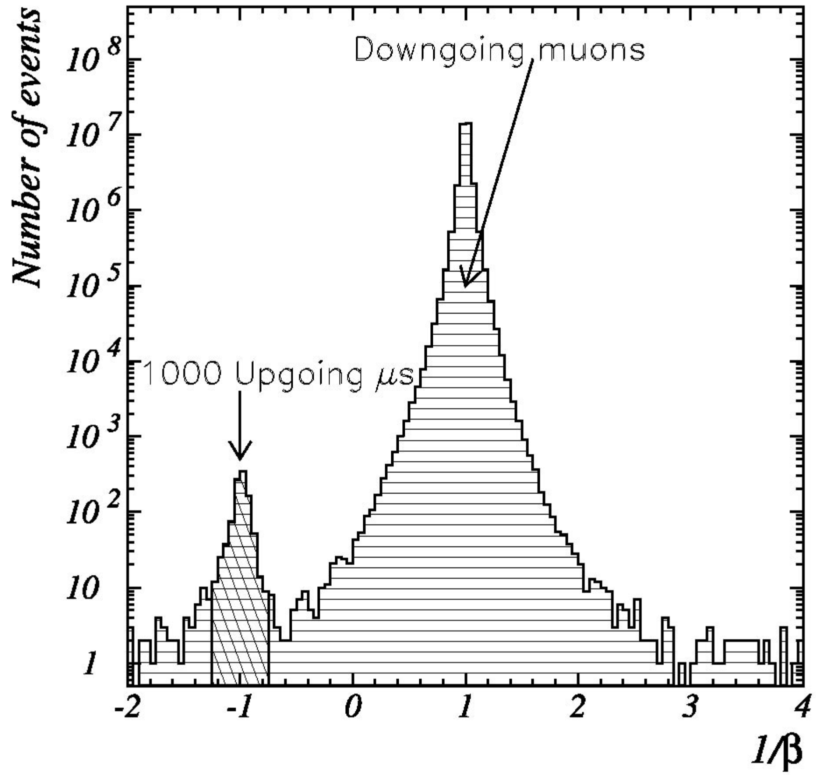

FIG. 2.—The $1/\beta$ distribution for the muon data sample collected with the full detector. The number of down-going muons is $\sim 33.8 \times 10^6$.

NEMO: Capo Passero

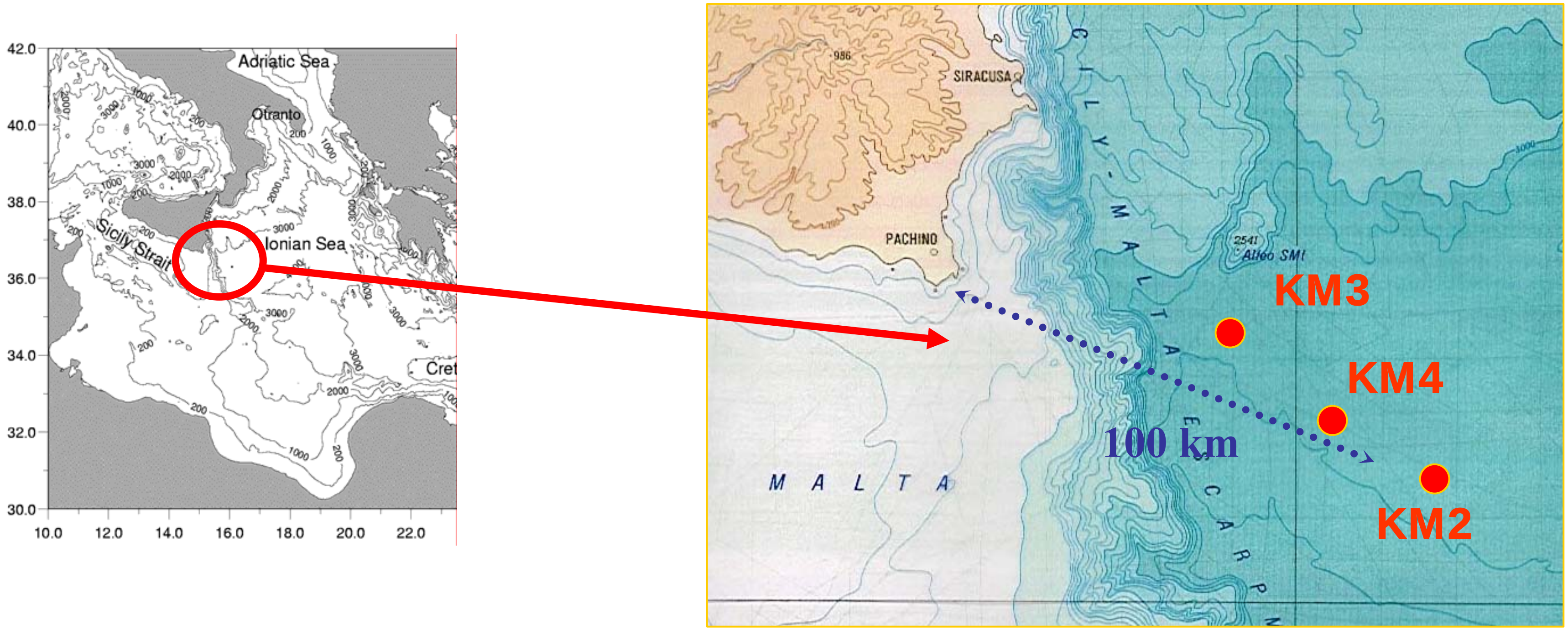

- **KM2 36°10’ N 16°19’E, depth 3350m (1: Jan ‘99)**
- **KM3 36°30’ N 15°50’E, depth 3345m (1: Feb ‘99, 1: Aug’99, 2: Dec ‘99)**
- **KM4 36°19’N, 16°04’E, depth 3341m (2: Dec ‘99, 2: March ’00, contiuing)**

Km3Net

The KM3NeT Project

Design Study for a Deep Sea Facility in the Mediterranean for Neutrino Astronomy and Environmental Sciences

Progetto approvato dalla Comunita' Europea (Novembre 2005)

9 MEuro

Progetto esecutivo di un rivelatore da 1 km3 nel Mediterraneo

(da completare in 3 anni)

Institutions

- Institutes participating in the Design Study:

Cyprus: ***Univ. Cyprus***

France: ***CEA/Saclay, CNRS/IN2P3 Marseille, CNRS/IN2P3 Strasbourg, Univ. Haute Alsace***

Germany: ***Univ. Erlangen***

Greece: ***Hellenic Open Univ., NCSR “Demokritos”, NOA/Nestor Inst., Univ. Athens, Univ. Crete, Univ. Patras***

Italy: ***INFN (Bari, Bologna, Catania, LNS Catania, LNF Frascati, Genova, Messina, Pisa, Roma-1)***

Netherlands: ***NIKHEF (Univ. Amsterdam, Free Univ., Univ. Utrecht, Univ. Nijmegen)***

Spain: ***IFIC (CSIC, Univ. Valencia), U.P. Valencia***

United Kingdom: ***Univ. Leeds, Univ. Sheffield, Univ. Liverpool***

Coordinator: Uli Katz, Erlangen